NEONICOTINOIDS

Neonicotinoid exposure disrupts bumblebee nest behavior, social networks, and thermoregulation

James D. Crall[1,2,3]*, Callin M. Switzer[4,5], Robert L. Oppenheimer[6], Ashlee N. Ford Versypt[7,8], Biswadip Dey[9], Andrea Brown[1], Mackay Eyster[10], Claire Guérin[11], Naomi E. Pierce[1], Stacey A. Combes[12], Benjamin L. de Bivort[1,3]

Neonicotinoid pesticides can negatively affect bee colonies, but the behavioral mechanisms by which these compounds impair colony growth remain unclear. Here, we investigate imidacloprid's effects on bumblebee worker behavior within the nest, using an automated, robotic platform for continuous, multicolony monitoring of uniquely identified workers. We find that exposure to field-realistic levels of imidacloprid impairs nursing and alters social and spatial dynamics within nests, but that these effects vary substantially with time of day. In the field, imidacloprid impairs colony thermoregulation, including the construction of an insulating wax canopy. Our results show that neonicotinoids induce widespread disruption of within-nest worker behavior that may contribute to impaired growth, highlighting the potential of automated techniques for characterizing the multifaceted, dynamic impacts of stressors on behavior in bee colonies.

Animal pollinators support biodiversity and agricultural yields (*1*, *2*), and there is growing concern over the causes and consequences of declining bee populations (*3*, *4*). Mounting evidence indicates that neonicotinoid pesticides can negatively affect both commercial honey bee (*5*, *6*) and wild bee (*7*) populations. Neonicotinoids are agonists of nicotinic acetylcholine receptors and therefore disrupt cholinergic signaling in the insect central nervous system. Neonicotinoids are believed to reduce growth of developing brood (*7*–*9*) by impairing foraging behavior [including navigation (*5*, *10*) and floral learning (*11*, *12*)], leading to reduced colony resource intake (*13*, *14*). Recent work, however, shows that neonicotinoid exposure can impair colony growth without altering foraging (*15*) [and vice versa (*16*)].

In addition to foraging, workers in social insect colonies perform critical tasks within the nest (e.g., larval incubation and feeding, cleaning, and nest construction) that are vital for colony development. Although nest workers are exposed to neonicotinoid residues (*7*, *17*) that may affect behavior [including physiology (*18*, *19*) and locomotion (*20*–*22*)], neonicotinoids' effects on within-nest behaviors are poorly understood.

To investigate imidacloprid's effects on bumblebee (*Bombus impatiens*) nest behavior, we combined a system for automated behavioral tracking of uniquely identified workers [BEEtag (*23*, *24*)] with a robotic observation platform (Fig. 1, A to C), allowing long-term (12-day, Fig. 1 and figs. S1 and S2) tracking of uniquely identified bumblebee workers and queens. Colonies were given ad libitum access to either pure nectar (control, $n = 9$), or nectar containing field-realistic concentrations of imidacloprid, a globally prevalent neonicotinoid [$n = 9$, 6 parts per billion (ppb)].

Chronic imidacloprid exposure impairs a suite of worker behaviors within the nest. Workers in imidacloprid-exposed colonies spent significantly less time active (Fig. 1D and fig. S2). Imidacloprid exposure also reduced rates of nursing among workers (Fig. 1E and fig. S2) and shifted spatial occupancy toward the nest periphery (Fig. 1F and fig. S2).

Behavioral effects of imidacloprid differed markedly between night and day [14:10 light:dark (L:D) cycle] within the colony (Fig. 1); reductions in activity were stronger at night (Fig. 1D and fig. S2) than during the day (but were significant during both night and day, see fig. S2) and effects on daytime activity declined over time (with effects undetectable by the end of the exposure period, Fig. 1D). Reductions in nursing and distance from the nest center were significant at night, but not during the day (Fig. 1, E and F, and fig. S2). Imidacloprid reduced social network density compared to controls, consistent with effects of thiacloprid in honey bees (*25*), although this effect was also only significant at night (Fig. 1G; network density, night: bootstrap $p = 0.0042$; network density, day: bootstrap $p = 0.71$). Imidacloprid increased movement speed in workers, although this effect appears delayed and is only significant during the day (fig. S2). Whereas previous work has shown that imidacloprid exposure can lead to either hyperactivity or immobility depending on dose (*26*), these results show that both effects can occur at the same concentration. Imidacloprid also reduced activity and nursing in queens (fig. S2), consistent with results in honey bees (*27*) and bumblebees (*28*, *29*). Body concentrations of imidacloprid measured after the experiment were independent of foraging activity, confirming that even nonforaging nest workers are exposed to imidacloprid (fig. S3, mean concentration = 2.25 fmol imidacloprid per milligram of body mass).

To confirm that imidacloprid induces direct and rapid changes in nest behavior after exposure, we recorded behavior of workers in four additional *B. impatiens* colonies on the days immediately before and after individually administered, acute consumption of 0 (control), 0.1, or 1.0 ng of imidacloprid (Fig. 2; see supplementary text for justification of doses).

Acute imidacloprid exposure altered nest behavior within 24 hours, with effects qualitatively similar to those of chronic exposure (Fig. 2 and tables S1 to S4). Bees fed 1.0 ng of imidacloprid had reduced activity and nursing, were located further from the nest center, and had reduced social interactions compared to controls (Fig. 2 and table S2). Bees fed 1.0 ng of imidacloprid showed reduced foraging, driven by a reduction in nonforagers initiating foraging after treatment—rather than a decrease in foraging among foragers (tables S2 to S4). Bees fed 0.1 ng of imidacloprid showed no significant differences in behavior compared to controls (fig. 2 and tables S1 to S4).

To gain insight into the mechanisms underlying the multiple behavioral outcomes of imidacloprid exposure, we developed a spatially explicit, agent-based model of worker nest movements (supplementary text and figs. S4 to S6). Bees were modeled as either active (moving) or inactive (not moving) at each time point and Markovian transitions were used to switch between these states (fig. S4). The transition rates were modulated by contact with nestmates and the bee's location on or off the nest and were directly estimated from experiments (fig. S5). When bees were active, they moved with a random walk biased toward the nest center (fig. S4; parameters also fit from experiments).

We then used this model to disentangle the effects of imidacloprid on activity, space use, and social interactions and found evidence that these multiple outcomes of imidacloprid exposure are functionally linked; simulations isolating imidacloprid's direct effects on activity (both spontaneously in isolated workers and when activity is modulated by social contact; fig. S5) resulted in shifts in spatial occupancy and interaction rate within the nest (fig. S6). These effects are

[1]Department of Organismic and Evolutionary Biology, Harvard University, Cambridge, MA, USA. [2]Planetary Health Alliance, Harvard University, Cambridge, MA, USA. [3]Center for Brain Science, Harvard University, Cambridge, MA, USA. [4]eScience Institute, University of Washington, Seattle, WA, USA. [5]Department of Biology, University of Washington, Seattle, WA, USA. [6]Department of Biological Sciences, University of New Hampshire, Durham, NH, USA. [7]School of Chemical Engineering, Oklahoma State University, Stillwater, OK, USA. [8]Interdisciplinary Toxicology Program, Oklahoma State University, Stillwater, OK, USA. [9]Department of Mechanical and Aerospace Engineering, Princeton University, Princeton, NJ, USA. [10]Biology Department, University of Massachusetts Amherst, Amherst, MA, USA. [11]Department of Ecology and Evolution, Université de Lausanne, Lausanne, Switzerland. [12]Department of Neurobiology, Physiology, and Behavior, University of California, Davis, Davis, CA, USA.
*Corresponding author. Email: jcrall@oeb.harvard.edu

compounded by imidacloprid's reduction of attraction to the nest center (fig. S6 and supplementary text).

To test neonicotinoids' effects on nest behavior under realistic conditions, we quantified nest thermoregulation performance in free-foraging *B. impatiens* colonies (Fig. 3, A and B). Colonies were given ad libitum access to nectar containing imidacloprid (6 ppb, n = 9) or pesticide-free nectar (n = 9) within the nest, but foraged outdoors to gather pollen. For each colony, we measured the surface temperature of the brood and air temperature within the nest chamber, in addition to outdoor air temperature (Fig. 3, A and B). Imidacloprid impaired thermoregulation of the developing brood (Fig. 3, C and D, and fig. S7, permutation test, p = 0.005, tables S5 and S6) and nest air temperature (Fisher's

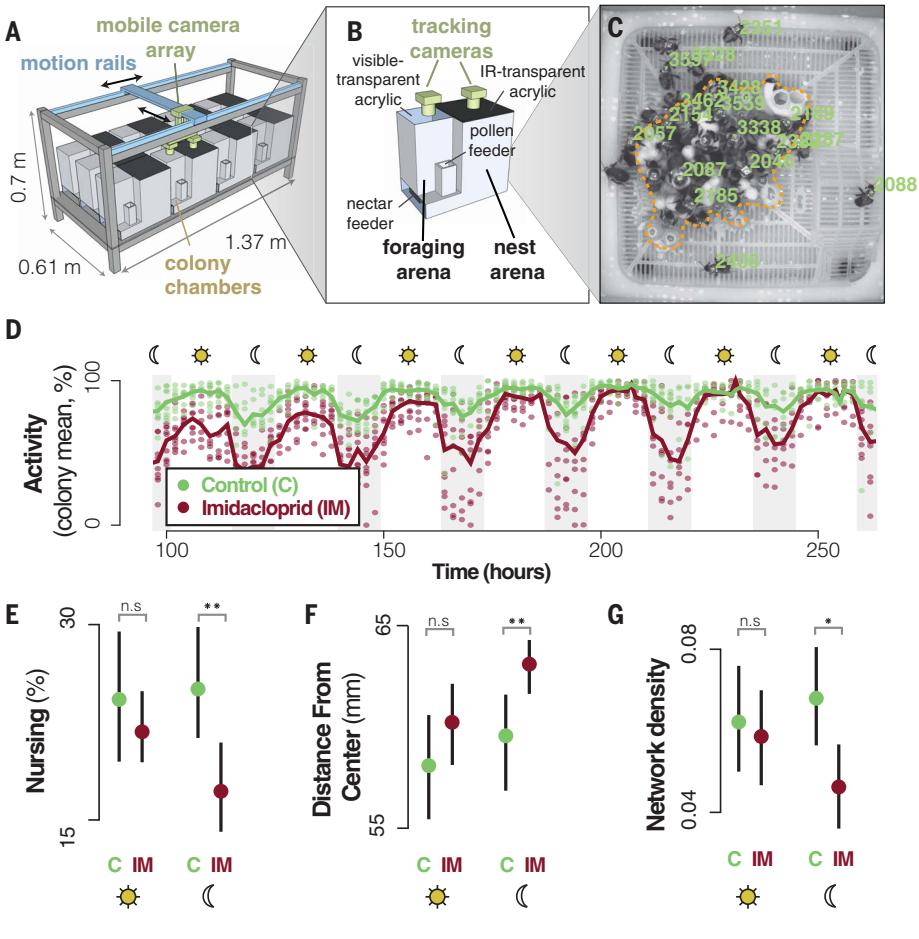

Fig. 1. Chronic exposure to imidacloprid alters nest behavior and social interactions in bumblebee colonies. (**A** and **B**) Schematic diagrams of (A) robotic platform for multicolony (in a 4 by 3 array) behavioral tracking and (B) a single colony chamber. (**C**) Example tracking of nest workers, with unique identification numbers shown in green. Orange dotted line shows the nest structure. (**D**) Colony mean percentage of time active over 7 consecutive days (with time indicating hours after exposure). Filled circles represent mean activity levels for a single colony (averaged across all individual workers) for a single 5-min trial, and solid lines show mean values for treatment groups (control colonies, n = 9, in green; imidacloprid-exposed colonies, n = 9, in red). Gray blocks and Sun/Moon symbols show the 14:10 hour L:D cycle in the tracking arena. (**E**) Percentage of time engaged in nursing. (**F**) Mean distance to the nest center and (**G**) social network density [proportion of possible pairwise interactions between workers that actually occur, during a single 5-min trial] by treatment group and time of day. *p < 0.05, **p < 0.005, based on 10,000 hierarchical bootstrap replicates. Solid markers in (E) to (G) show group means, and black bars indicate 95% bootstrap confidence intervals, with control and imidacloprid-exposed colonies shown in green and red, respectively. n.s., not significant.

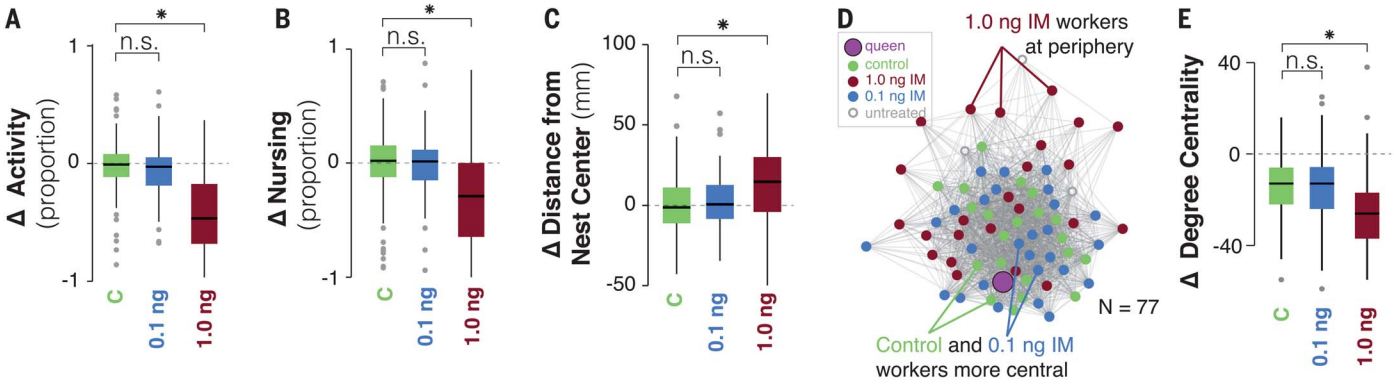

Fig. 2. Effects of imidacloprid on nest behavior occur rapidly after acute exposure. Changes in (**A**) activity, (**B**) nursing, and (**C**) distance from nest center of workers after exposure to different imidacloprid treatments. (**D**) Social network diagram of a representative colony, with nodes positioned by a force-directed algorithm. Circles represent individual bees, with gray lines drawn between bees that interacted during a 1-hour trial. The queen is shown as a purple circle, and untreated workers are shown as open gray circles. (**E**) Change in degree centrality (i.e., number of unique social interactions) after exposure by treatment. Boxplots show median (thick black lines), interquartile range (solid box), and range (thin lines, 75th and 25th percentile ± 1.5 × IQR), with outliers shown in gray. Behavioral changes were calculated as the difference in individual behavior 24 hours after versus 24 hours before exposure. In all panels, workers exposed to 1.0, 0.1, or 0 ng of imidacloprid are shown in red, blue, and green, respectively. *p < 0.001. n.s., not significant.

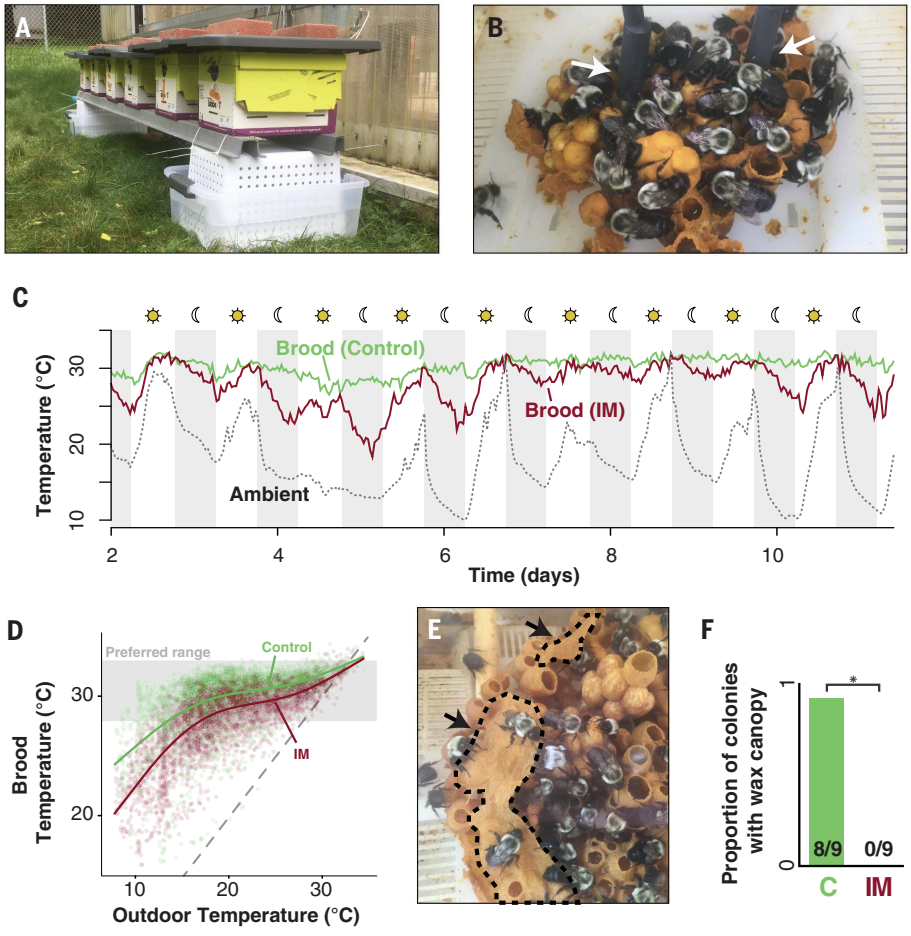

Fig. 3. Chronic imidacloprid exposure disrupts brood thermoregulation in *Bombus impatiens*. (**A**) Outdoor *B. impatiens* colonies with digital temperature sensors (**B**) (white arrows). (**C**) Example brood (solid lines) temperatures from one imidacloprid-exposed colony (red, IM) and one control (green, C) colony. Dotted line shows outdoor air temperature. (**D**) Brood versus outdoor temperatures for control (C, green) and treated (IM, red). Transparent markers show individual measurements across all colonies, and solid lines show LOESS-smoothed trends by treatment. Dashed line: brood temperature = outdoor temperature. (**E**) Example of a partially constructed insulating wax canopy (black arrows and dashed lines) covering brood cells. (**F**) Proportion of colonies that had a partially or completely constructed wax canopy by the end of the experiment, by treatment. Asterisk indicates significant difference between groups (p = 0.0005, permutation test).

exact test, p = 0.009, tables S5 and S6), with stronger effects occurring at lower temperatures (Fig. 3D). This result confirms that neonicotinoids' effects on thermogenesis in individual, isolated honey bees (*18*) and bumblebees (*19*) extend to colony temperature regulation under field conditions. We found a significant interaction between exposure and the direction of temperature change, suggesting that the effect of imidacloprid on thermoregulation may be stronger when air temperature is rising (fig. S7 and tables S5 and S6). Imidacloprid-treated colonies were also less likely to construct an insulating wax canopy around the developing brood, an important behavioral adaptation to cold (*30*) (Fig. 3, E and F, permutation test, p = 0.0005).

Large-scale field studies have revealed that the impacts of neonicotinoids on bee colonies can vary substantially depending on environmental context (*6*, *7*), highlighting the need for improved understanding of the mechanisms by which neonicotinoids affect workers and colonies. Our results suggest that reduced brood growth in neonicotinoid-exposed colonies (*7*) could result from impaired nursing behavior and temperature control by nest workers, in addition to reduced colony resource intake (*13*, *14*). These results support previous findings that neonicotinoids impair worker hygienic behavior in honey bees at higher concentrations [e.g., 50 ppb or higher (*27*)] and over extended exposure periods [e.g., 12 weeks (*31*)].

Our results highlight the multifaceted behavioral impacts of neonicotinoid exposure; imidacloprid's effects on nest behavior vary substantially with time of day (Fig. 1 and fig. S2), exposure affects both mobility and sensory decision-making (Figs. 1 and 2, fig. S5, and supplementary text), and the impacts of imidacloprid on brood thermoregulation are nonlinear (Fig. 3 and tables S5 and S6) and dynamic (fig. S7 and tables S5 and S6). These results illustrate the potential of high-throughput, automated analysis for improving our understanding of the context-specific effects of neonicotinoids, as well as efficiently screening agrochemicals more generally for sublethal impacts on pollinators.

REFERENCES AND NOTES

1. A. M. Klein *et al.*, *Proc. Biol. Sci.* **274**, 303–313 (2007).
2. N. Myers, *Proc. Natl. Acad. Sci. U.S.A.* **93**, 2764–2769 (1996).
3. G. K. Meffe, *Conserv. Biol.* **12**, 8–17 (1998).
4. N. Gallai, J.-M. Salles, J. Settele, B. E. Vaissière, *Ecol. Econ.* **68**, 810–821 (2009).
5. J. Fischer *et al.*, *PLOS ONE* **9**, e91364 (2014).
6. B. A. Woodcock *et al.*, *Science* **356**, 1393–1395 (2017).
7. M. Rundlöf *et al.*, *Nature* **521**, 77–80 (2015).
8. P. R. Whitehorn, S. O'Connor, F. L. Wackers, D. Goulson, *Science* **336**, 351–352 (2012).
9. R. J. Gill, O. Ramos-Rodriguez, N. E. Raine, *Nature* **491**, 105–108 (2012).
10. M. Henry *et al.*, *Science* **336**, 348–350 (2012).
11. D. A. Stanley, K. E. Smith, N. E. Raine, *Sci. Rep.* **5**, 16508 (2015).
12. K. Tan *et al.*, *Sci. Rep.* **5**, 10989 (2015).
13. R. J. Gill, N. E. Raine, *Funct. Ecol.* **28**, 1459–1471 (2014).
14. H. Feltham, K. Park, D. Goulson, *Ecotoxicology* **23**, 317–323 (2014).
15. A. N. Arce *et al.*, *J. Appl. Ecol.* **54**, 1199–1208 (2016).
16. D. A. Stanley, A. L. Russell, S. J. Morrison, C. Rogers, N. E. Raine, *J. Appl. Ecol.* **53**, 1440–1449 (2016).
17. E. A. D. Mitchell *et al.*, *Science* **358**, 109–111 (2017).
18. S. Tosi *et al.*, *J. Insect Physiol.* **93-94**, 56–63 (2016).
19. R. Potts *et al.*, *J. Insect Physiol.* **104**, 33–39 (2018).
20. S. M. Williamson, S. J. Willis, G. A. Wright, *Ecotoxicology* **23**, 1409–1418 (2014).
21. P. Medrzycki, R. Montanari, L. Bortolotti, S. Maini, C. Porrini, *Bull. Insectol.* **56**, 59–62 (2017).
22. S. Tosi, J. C. Nieh, *Sci. Rep.* **7**, 15132 (2017).
23. J. D. Crall, N. Gravish, A. M. Mountcastle, S. A. Combes, *PLOS ONE* **10**, e0136487 (2015).
24. J. D. Crall *et al.*, *Nat. Commun.* **9**, 1201 (2018).
25. N. Forfert, R. F. A. Moritz, *J. Apic. Res.* **56**, 467–474 (2017).
26. M. Lambin, C. Armengaud, S. Raymond, M. Gauthier, *Arch. Insect Biochem. Physiol.* **48**, 129–134 (2001).
27. J. Wu-Smart, M. Spivak, *Sci. Rep.* **6**, 32108 (2016).
28. M. Leza, K. M. Watrous, J. Bratu, S. H. Woodard, *Proc. Biol. Sci.* **285**, 20180761–20180769 (2018).
29. G. L. Baron, N. E. Raine, M. J. F. Brown, *Proc. Biol. Sci.* **284**, 20170123 (2017).
30. J. G. Holland, A. F. G. Bourke, *Funct. Ecol.* **29**, 1209–1217 (2015).
31. N. Tsvetkov *et al.*, *Science* **356**, 1395–1397 (2017).
32. J. D. Crall, C. M. Switzer, R. L. Oppenheimer, A. N. Ford Versypt, B. Dey, A. Brown, M. Eyster, C. Guérin, N. E. Pierce,

S. A. Combes, B. L. de Bivort, Neonicotinoid exposure disrupts bumblebee nest behavior, social networks, and thermoregulation. Zenodo (2018).

ACKNOWLEDGMENTS

We thank C. Vidoudez for help in chemical analysis; D. Zucker for help in the design of the robotic testing platform; and S. Donoughe, A. Kao, and members of the Pierce, Combes, and de Bivort labs, as well as three anonymous reviewers, for insightful comments on drafts of this manuscript. **Funding:** This material is based on work supported in part by BioBest, a National Science Foundation Graduate Research Fellowship (J.D.C.), a Winslow Foundation grant (J.D.C), funding from the Rockefeller Foundation (J.D.C.), the National Defense Science and Engineering Graduate Fellowship (NDSEG) Program (C.M.S.), UW Data Science Grant from the Moore and Sloan Foundations (C.M.S.), AFOSR grant FA9550-14-1-0398 (C.M.S.), National Science Foundation grant (CAREER IOS-1253677) to S.A.C., and NSF OIS-1257543 to N.E.P. B.L.dB. was supported by a Sloan Research Fellowship, a Klingenstein-Simons Fellowship Award, and the National Science Foundation under grant no. IOS-1557913. Modeling work by J.D.C., A.N. F.V, and B.D. was supported in part by workshop funding ("Data-Driven Modeling of Collective Behavior and Emergent Phenomena") from the Statistical and Applied Mathematical Sciences Institute (SAMSI). **Author contributions:** J.D.C., C.M.S., N.E.P., S.A.C., and B.L.dB. designed experiments. J.D.C, R.L.O., and C.M.S. performed acute exposure experiments. J.D.C., C.G., and B.L.dD. designed and constructed the robotic tracking arenas and platform. J.D.C., R.L.O., C.M.S., A.B., and M.E. collected data and performed experiments. J.D.C. performed automated tracking, behavioral analysis, and prepared solutions for chronic behavior and field experiments. J.D.C., A.N.F.V, and B.D. designed and implemented the agent-based model. C.M.S. mixed the solutions of imidacloprid for acute experiments and performed statistical analysis for acute experiments and thermoregulation experiments. C.M.S. and J.D.C. performed statistical analysis for chronic imidacloprid experiments. All authors wrote the manuscript. **Competing interests**: The authors declare no competing interests. **Data and materials availability:** Associated data and custom scripts are deposited at Zenodo (*32*).

SUPPLEMENTARY MATERIALS

www.sciencemag.org/content/362/6415/683/suppl/DC1
Materials and Methods
Supplementary Text
Figs. S1 to S12
Tables S1 to S6
References (*33*–*54*)
Movies S1 to S3

23 February 2018; accepted 26 September 2018
10.1126/science.aat1598

Science

Neonicotinoid exposure disrupts bumblebee nest behavior, social networks, and thermoregulation

James D. Crall, Callin M. Switzer, Robert L. Oppenheimer, Ashlee N. Ford Versypt, Biswadip Dey, Andrea Brown, Mackay Eyster, Claire Guérin, Naomi E. Pierce, Stacey A. Combes and Benjamin L. de Bivort

Science **362** (6415), 683-686.
DOI: 10.1126/science.aat1598

Trouble at the hive

Neonicotinoid pesticides cause mortality and decline in insect pollinators. One repeatedly noted effect is a reduction in bee colony size. However, the mechanism behind this reduction is unclear. Crall *et al.* performed complex real-time monitoring of bumblebee behavior within their nests (see the Perspective by Raine). Neonicotinoid exposure reduced nurse and caretaking behaviors, which affected productivity and harmed colony thermoregulation. These changes in behavior acted together to decrease colony viability, even when exposure was nonlethal.

Science, this issue p. 683; see also p. 643

Science (print ISSN 0036-8075; online ISSN 1095-9203) is published by the American Association for the Advancement of Science, 1200 New York Avenue NW, Washington, DC 20005.

www.sciencemag.org/content/362/6415/683/suppl/DC1

Supplementary Materials for

Neonicotinoid exposure disrupts bumblebee nest behavior, social networks, and thermoregulation

James D. Crall*, Callin M. Switzer, Robert L. Oppenheimer, Ashlee N. Ford Versypt, Biswadip Dey, Andrea Brown, Mackay Eyster, Claire Guérin, Naomi E. Pierce, Stacey A. Combes, Benjamin L. de Bivort

*Corresponding author. Email: jcrall@oeb.harvard.edu

Published 9 November 2018, *Science* **362**, 683 (2018)
DOI: 10.1126/science.aat1598

This PDF file includes:

Other Supplementary Materials for this manuscript include the following:
(available at www.sciencemag.org/content/362/6415/683/suppl/DC1)

Movies S1 to S3

Materials and Methods

Data and code

Custom code and all data after processing of raw videos are available on zenodo.org(*32*). A repository of custom code will also be maintained and updated at https://github.com/jamescrall/beeTracking.

Chronic Exposure Nest Behavior Experiments

Arena design and experimental outline

Eighteen queenright commercial bumblebee colonies (*Bombus impatiens*, BioBest®) containing on average 32.2 (± 7.6, s.d.) workers were CO_2-anaesthetized and removed from the colony. Each bee, including the queen, was outfitted with a unique BEEtag(*23*) printed on waterproof, tear-resistant paper. Tags measured 3x4 mm and weighed roughly 2.4 mg each. Tags were affixed to the mesoscutum of each bee with cyanoacrylate glue (super glue gel, ACE, Oak Brook Il).

After tagging, bees were transferred, along with all nest structure and brood, to a custom-made tracking arena for behavior observation (Fig 1). Each colony arena consisted of a nest arena (0.18 m x 0.18 m) and a foraging arena (0.18 m x 0.12 m) constructed of opaque white acrylic (3 mm thick) with narrow (1.5 mm) ventilation slits running along their length at 1-inch intervals to allow for air circulation but prevent bees from escaping. One wall of the foraging chamber was constructed of clear acrylic to allow observation and manipulation (Fig 1B). The ceiling of each chamber was constructed of clear (i.e., transparent to visible light) acrylic sheets, and the nest chamber was covered with an additional sheet of visually opaque, near-infrared transparent acrylic, allowing this arena to remain visually dark to bees (simulating the natural light environment of ground-nesting of *B. impatiens*) but transparent to IR-sensitive cameras (see below).

Each colony was then relocated to a randomly-assigned position on a robotic tracking platform (Fig 1A, capacity = 12 colonies, see "Robotic tracking platform and trial structure" below for details of trial structure) with ad-libitum access to a gravity-fed dry pollen feeder through a metal screen and a nectar feeder (i.e., a nectar reservoir with a wick) containing either control artificial nectar or nectar containing imidacloprid (see below). We performed these experiments on indoor (rather than free-foraging) colonies to provide complete control over neonicotinoid exposure. Nectar consumption was measured for each colony by successively weighing the mass of the removable nectar reserve (adjusting for evaporation based on baseline evaporation measurements in identical nectar reservoirs but in a chamber without bees), and per adult consumption rates were estimated by dividing this value by the number of individuals in the colony (estimated by averaging the number of live individuals at the beginning and end of the experimental trial period). All colonies recovered activity quickly (within 30 minutes) after CO_2 exposure, and initiated foraging within 24 hours. Data recording was initiated within 5 hours after colonies were transferred to tracking arenas.

Robotic tracking platform and trial structure

Videos for behavioral analysis were recorded using a robotic-gantry system suspended above the colony platform (Fig 1A, Movie S1)(*33*). The gantry carried two IR-sensitive cameras; a Point Grey® Black monochrome 2448x2048 USB 3.0 video camera and a Chameleon monochrome 1268x964 USB 3.0 video camera for recording behavior in the nest and foraging chambers, respectively. The gantry also housed a custom-designed IR-LED array for tracking

illumination, controlled by custom Matlab scripts via an Arduino microcontroller. The camera gantry was positioned within the tracking platform using stepper motors to slide two carriages on Cartesian rails using belts and pulleys in a CoreXY arrangement (corexy.com). Stepper motors were controlled using a Smoothieboard motion controller board via custom Matlab script. Custom Matlab scripts were written to move the camera gantry to known colony positions and record 5-minute video trials every two hours over 12 days after colonies were transferred. Colonies were tested in three "cohorts" of 6 colonies each (with 3 treated and 3 control colonies) staggered by ~one week (i.e., experiments began for cohorts 1, 2, and 3 on March 17, March 24, and March 30 2018, respectively). The timing of tagging and transfer (1 day) and exposure (12 days) were identical for each cohort.

Image processing and nest behavior analysis

To automate the analysis of worker behavior within nests, we developed a custom computational pipeline in Matlab. Unless otherwise noted, all analyses below were performed using this automated approach.

To increase processing speed, a background image for each colony (for each day) was calculated as the median intensity over time for each pixel, using an evenly spaced subsample of 5 frames from each video collected. Frame regions that did not contain bees were automatically removed (i.e., converted to black) by intensity thresholding against this background, and subsequently eroded and dilated. Segmented images were examined for BEEtags using optimized adaptive thresholding parameters, yielding tag locations of tracked bees for each frame. Missing track data were "healed" using linear interpolation for missing sections up to ~2 seconds, and all other gaps were left as missing values. Bees were considered mobile when movement speed exceeded a threshold derived from the bimodal distribution of speeds (see below).

Nest structures were outlined for each colony on each day using a semi-automated custom Matlab script, and digitally dilated to define a boundary within one cm of nest structures. Bees were considered "nursing" when they were physically located on or within one cm of the nest structure. Previous work has shown that this approach for automatically classifying nursing behavior has strong agreement with manually-identified behaviors(*24*). Specifically, reanalysis of the data from (*24*) (Supplementary Table 2 in that paper) shows that bees located within one cm of the nest structure were correctly identified 93% (overall unbalanced accuracy) of the time as performing one of several nursing behaviors (including incubating, anchoring pots, inspecting and cleaning pots, among others), as opposed to other behaviors not associated with direct nursing (including patrolling, resting, and perching), using established behavioral categories for bumblebees(*34*, *35*). It is important to note that larval feeding is difficult to identify from these video data, and thus it is not possible to reliably infer rates of larval feeding from our automated behavioral classification.

Bees were recorded as "foraging" when they were located within ~1 body length (specified by a manually-drawn ROI) around the nectar and pollen feeders in the foraging chamber. This approach had strong agreement (94.2% overall unbalanced accuracy) with manual identification of feeding behavior by a blinded observer. For each trial, the social center of the colony was defined as the mean of all 2d coordinates from all bees tracked within the nest during that trial, and distance to social center was calculated as the mean instantaneous distance from this point for each bee.

To estimate effects of imidacloprid on social networks, we used spatial distance between workers as a proxy for physical contact. Physical contact is an important (though not exclusive) component of social communication within bumblebee colonies(*36*) and has previously been shown to predict disease transmission dynamics within colonies(*37*). Workers were considered interacting when distance to another worker (between tag centroids) was below one cm (roughly a bee body length). Previous work has shown that this threshold is an accurate proxy for physical contact in *Bombus impatiens*(*37*). To assess the accuracy of this threshold in our experiments, an observer (blinded to the automated interaction scoring) manually scored 1000 randomly sampled pairs of potentially interacting (i.e. located within 3.0 cm of each other) workers for physical contact (including touching appendages and antennation). A 1.0 cm threshold correctly categorized 83% of these potential interactions (overall unbalanced accuracy), with a false positive (i.e., when bees were incorrectly identified as interacting based on spatial proximity) rate of 1.2%. Consistent with previous work, we thus find that this spatial proximity threshold provides a conservative proxy for physical contact among nestmates in *Bombus impatiens*.

Social network density within the nest was estimated for each trial by calculating the proportion of potential network connections (i.e., all pairs of bees that were tracked during that trial) that were actually observed (i.e., those two bees physically interacted during the trial).

Statistical analyses

Effects of chronic imidacloprid exposure on behavioral metrics (i.e., activity level, nursing, distance from center, and network density) were estimated using a hierarchical bootstrapping approach. For each bootstrap replicate, colonies were resampled with replacement and the difference in each behavioral metric (between treatment and control groups) was averaged across all trial time periods (measured continuously from the beginning of the experiment) to account for variation both within and across days. Mean effects and 95% confidence intervals were estimated from the distribution from 10,000 bootstrap replicates. P-values were calculated from the distribution of between-treatment differences in the mean for each metric across bootstrap replicates. The fraction of resampled effect size estimates was taken as the p-value for the 2-tailed test. Uncorrected p-values are reported here and throughout the manuscript unless otherwise noted.

For all analyses of chronic exposure experiments, separate models were built for day and night periods, based on when the arenas were lit (14:10 L:D cycle from, with lights on from 5 am to 7 pm). Several nest behavioral metrics showed trends throughout the experimental period in both control and treatment groups, particularly during the first ~4 days of the experiment (Fig S1), which appear unrelated to drift in automated tracking performance over time (Fig S8). While all statistical models account for variation over time and across days, we ran separate models for each metric excluding the first four experimental days. Qualitative results for most metrics in separated day/night periods were similar between models including and excluding the first four experimental days (Fig S2), with the exception of moving speed in workers (which showed a significant increase in treated colonies during the day only when the acclimation period was excluded), and night-time activity in queens (which showed a significant reduction in imidacloprid-exposed colonies only when the acclimation period was included, $p < 0.05$, hierarchical bootstrap).

To examine potential variable effects of imidacloprid over time, we additionally ran separate analyses of all behavioral metrics (excluding the acclimation period of the first 4 experimental days) over the entire exposure period. We found evidence that imidacloprid's effects diminished over the exposure period for daytime activity and daytime foraging, with the

differences between experimental and control groups decreasing over time for these two metrics (these and further figures available on zenodo.org(*32*)). As exposure was constant during these experiments, differences over time in these metrics could result from changes with age of marked workers (since new workers were not marked progressively during the experimental trials)(*35*), group size(*27*) (as new workers emerged and colonies grew during the experimental period), or physiological adaptation/acclimation. We found no evidence that imidacloprid's effects substantially differed with time of exposure for any behavioral metrics other than daytime activity or daytime foraging.

We also examined differential effects of imidacloprid across the three experimental cohorts, and found no evidence that imidacloprid's effects on any behavioral metric varied significantly across these experimental cohorts.

Imidacloprid solution preparation and confirmation

Treated nectar solutions were prepared by dissolving 5.0 mg of analytic standard imidacloprid (PESTANAL®, Sigma-Aldrich) in 50 mL dH_20, and then transferring 30 µL aliquots of this concentrated solution into 500 mL of artificial nectar (Biogluc®) to achieve final concentration of 6 ppb. Seven samples of these final stock solutions (with one, three, and three samples taken from three technical replicates, respectively) were analyzed by LCMS (see below) to confirm the dosing concentration, with a mean concentration of 5.34 ppb (+/- 0.29 SE), within the approximate LC/MS instrument error of 20% at these concentrations. Solutions were stored in the dark, because imidacloprid is broken down by aquatic photolysis(*38*).

Imidacloprid body concentration

Whole-body mean imidacloprid concentrations were analyzed for bees from three treated and three control colonies from a single experimental cohort. For treated colonies, the queen and seven tagged workers were selected at random at the end of the experimental period (between 1 pm and 4 pm) and analyzed separately. For control colonies, four workers were randomly sampled and pooled from each colony. Samples were prepared following the method described in Cresswell *et al.*(*39*). In short, bees were transferred one by one to a screw cap plastic vial. To each sample, 1 ml of 25% methanol and 20 µl of internal standard (d4 imidacloprid, 500nM in methanol) were added. Two metal beads (2.4mm) were added to each sample and all samples were processed in a Fastprep-24 5G bead beater (Mobio), at 10 m/s for 2x 120 secs. Samples were then centrifuged at 16000 rpm for 10min, and 900 µl of supernatant was transferred to new 2ml Eppendorf tubes. 900 µl of 25% acetic acid in water was then added to each sample. Samples were then purified by solid phase extraction (SPE, DSC-18 1ml, 50mg from Supelco®) as follows: SPE cartridge were conditioned with 1 ml methanol, and washed with 1 mL water. 600 µl of sample was loaded on each cartridge. The cartridges were then washed with 1 ml of water and dried, and samples were eluted with 4 x 200µl methanol. Eluates were dried in glass vial, under nitrogen flow at 30°C. After resuspension in 40µl acetonitrile, the samples were transferred to microinserts and run on a Liquid Chromatography Mass Spectroscopy core facility machine.

Liquid chromatography/Mass spectrometry analyses

A standard curve was prepared as a 1 to 5 dilution series covering all concentrations encountered and extracted using the same protocol as the bees. Samples were analyzed on Agilent 6460 Triple Quad mass spectrometer coupled with Agilent 1290 Infinity and with a

Kinetex 2.6 µm C18 100 Å, 150x2.1 column. The mobile phases were A: water with 0.1% formic acid and B: Acetonitrile with 0.1% formic acid. The gradient started with 4 min at 0% B, then increased to 100% B over 10 min. After maintaining 100% for 4 min, the system was brought back to original conditions and equilibrated for 4 min. The flow rate was maintained at 0.3 mL / min, and the column was heated to 35°C. Imidacloprid was detected by two transitions in the MS (256.1 to 209 as quantifier and 256.1 to 175 as qualifier) and Imidacloprid-D4 was detected using 260.1 to 213 as quantifier and 260.1 to 179 as qualifier.

Acute Exposure Experiments

Arena design and experimental outline

Four colonies of bumblebees (*Bombus impatiens*) were acquired from BioBest® between Nov 1st and Dec 5th 2015. Colonies contained between 90 and 130 workers. Two colonies (Colonies A and C) had a small number of males (11 and 5, respectively), which were removed before any experimental trials began. Each colony was transferred to a custom nest box (Fig. S9, 0.20 x 0.19 x 0.13 m). The walls and floor of the nest box were constructed from black, extruded acrylic (6.3 mm thick). The walls and floor both had 1.6 mm-wide perforations running along their length at 25 mm intervals to allow for air circulation but not let bees escape. The top of the nest box was constructed from clear, laser-cut extruded acrylic (3.1 mm thick) to allow for imaging. A monochrome digital camera (DMK 24UJ003, USB 3.0, Imaging Source, 3856 x 2764 pixels) with a wide-angle lens (Fujinon, 2.8-8 mm) was mounted on extruded aluminum rails (25 mm, Thorlabs®) above the clear top of the nest box. The nest was illuminated with two 150mm x 150mm arrays of red LEDs (Knema Lighting®) spaced in a 20 mm grid, which are unlikely to influence nest behavior since bees have poor sensitivity to red light(*40*). The nest box, camera, and lighting array were covered with black cloth to exclude room light (Fig. S9).

After transferring all bees and the nest structure (including brood and honeypots, which were removed from shipping boxes along with the plastic platform on which these nest structure were built), colonies were allowed to acclimate to the nest box for 72 hours, where they were provided with ad libitum pollen and nectar directly within the nest.

After the acclimation period, colonies were given access to a clear plastic tunnel that ran roughly 0.5 meters from the nest to the foraging chamber (Fig. S9), which was a 0.8 m x 0.6 m x 0.6 m screened enclosure within the lab. Bees could access the tunnel through a 1 cm (diameter) hole in one wall of the nest box. The foraging chamber was illuminated with four 150-watt incandescent lights maintained on 12h light, 12h dark cycle from 9 am to 9 pm. Once colonies had access to the foraging chamber, they were no longer supplied with nectar or pollen within the nest.

An artificial feeder constructed of white, laser-cut extruded acrylic (3.1 mm thick) was located on the far wall of the foraging chamber, supplying the bees with ad libitum access to artificial nectar (Biogluc®) and pollen (Koppert®). The feeder was divided by a 2 cm-high wall that separated the nectar supply on one side from the pollen supply on the other. The feeder could be refilled from outside of the enclosure (Fig. S9); the nectar supply was replenished when necessary, and the pollen feeder was cleaned and refilled daily. Bees had direct access to the pollen supply and access to the nectar via a wick. A monochrome digital camera (Chameleon3, USB 3.0, Point Grey®, 1288 x 964 pixels, Fujinon 2.8-8 mm lens) was mounted roughly 15 cm above the feeder.

Colonies were allowed to acclimate to the foraging chamber for 72 hours, after which all bees were removed from the foraging chamber and the nest and cold-anaesthetized at 4°C for 1-2

hours. Bees that remained active were cooled at -11°C for about 1 minute prior to tagging. All bees (including the queen) were marked with unique BEEtags as described above. Each bee was then weighed and returned to the nest box.

After being returned to the nest, bees were allowed to forage undisturbed for 48 hours, during which time initial (i.e., pre-treatment) nest behaviors and foraging activity were recorded (see below). After 48 hours, all tagged bees (excluding the queen, newly eclosed workers, or bees that had lost their tags) were removed from the nest box and foraging chamber and cold-anaesthetized for 30 minutes at 4°C, then separated into individual, breathable plastic containers and starved (i.e., deprived of both nectar and pollen) for 2 hours to encourage subsequent feeding. Individual bees were then hand-fed (using a micropipette) 10 μL of artificial nectar containing one of three randomly assigned dosages (see below). Bees were maintained in separate chambers for an additional hour to ensure full consumption of nectar/imidacloprid solutions and to prevent regurgitation of treatment solutions into shared honeypots within the nest. Following this additional starvation period, all bees were returned to the nest box, except for the few bees that died during this procedure (less than 3% of bees treated, potentially due to individual variation in feeding status upon removal from the colony).

Colonies were then given undisturbed access to the foraging chamber for an additional 48 hours, during which time post-treatment nest behavior and foraging activity were recorded. After 48 hours, all bees were removed from the hive. The same process was repeated for subsequent colonies, after cleaning the nest box, foraging tube, and artificial feeder with water.

Preparation of solutions and experimental exposure

We dissolved 0.0040 g of imidacloprid (Pestanal, Sigma-Aldrich, St. Louis, Missouri) in 20 mL of deionized water to produce an initial concentration of 0.2 g L^{-1}. We then performed a series of 1/10 dilutions to arrive at concentrations of 200 μg L^{-1} and 20 μg L^{-1}. Immediately before treating bees, we mixed the imidacloprid solutions with sugar water (Biogluc®, BioBest, Westerlo, Belgium) in equal parts. Thus, the final concentrations fed to bees were 100 μg L^{-1} and 10 μg L^{-1} imidacloprid mixed in sugar water. The density of a 50% Biogluc®/50% water solution is approximately 1.15 kg L^{-1}, which allows us to convert the concentrations to ppb (w/w). The final concentrations of imidacloprid fed to bumblebees were approximately 8.7 ppb (μg kg^{-1}) and 87 ppb.

We fed each bee 10 μL of solution containing one of three doses of imidacloprid. The control dose was 50% Biogluc® and 50% water with no imidacloprid. The treated bees consumed 10 μL of either 100 μg L^{-1} or 10 μg L^{-1} imidacloprid in sugar water, which translates to each bee consuming either 0.1 ng or 1 ng of imidacloprid.

Image acquisition and tracking software

Nest behavior and foraging activity were recorded on the day before and the day after treatment. For nest behavior, a single, 1-hour video was recorded to a laptop computer (Dell Latitude E6530, 2.60 GHz i7 Intel Processor, 8 GB RAM) at 2 Hz using IC Capture (Imaging Source®). Video recordings were started at 2 pm on each day of data collection, and red lights were turned on for at least 20 minutes before recording began to allow bees to habituate, as a precaution to allow for habituation in the case that bees were able to perceive the red light. Each video frame was analyzed using BEEtag software(*23*), and the identities and coordinates of every tag in the frame were recorded (Fig S10, Movie S2). This approach yields a very low incorrect

positive identification rate, with no false positives (either a tag identified with the incorrect number, or a non-tag section of the image identified as a tag) detected among 2543 manually-inspected tag readings. Spatial coordinates for each bee were corrected for lens distortion using the Camera Calibration toolbox during post-processing in Matlab. Gaps of missing coordinates of up to 5 seconds were linearly interpolated.

Foraging behavior was continuously monitored (using motion detection) when lights were on in the foraging chamber (12:12 L:D cycle), using the camera mounted directly above the feeder. A video feed from the camera was monitored using custom scripts in Matlab on the same Dell laptop computer described above. Each time motion was detected on the feeder, a single image was recorded and processed using BEEtag. The identity and coordinates of any identified tags were recorded and the motion capture was started again after a 5-second delay (Movie S3).

Analysis of nest behavior

We measured six aspects of in-nest behavior, again using a fully automated computational pipeline (unless otherwise noted). (1) we calculated the proportion of time each bee was active by dividing the number of frames in which a bee was moving by the number of time steps over which its movement speed could be calculated (i.e., when a bee's tag was detected in two subsequent video frames). Bees were considered to be "inactive" if the movement speed of their tag was below 0.13 mm s^{-1}. This threshold was chosen based on the bimodal distribution of instantaneous speeds within the nest, the lower mode of which is likely due primarily to tag position measurement error rather than real movement of bees (Fig. S11).

(2) We calculated the proportion of time each bee spent nursing by dividing the number of frames a bee was detected on the nest by the total number of frames in which that bee was detected. Bees were considered to be on the nest if they were found within 1 cm (roughly one body length) of any part of the nest structure. The boundary of the nest structure was digitized by hand, and then corrected for lens distortion and scaled following the same procedure performed for all bee spatial coordinates within the nest. (3) We measured active speed by calculating the average speed of each bee, over the frames when they were active (i.e., when their instantaneous speed was above 0.13 mm s^{-1}). (4) We measured the average distance of a bee from the queen, over the frames in which that bee was identified. (5) We measured distance of each bee from the hive center, by first calculating an average "social center" of the hive (i.e., the mean of all x and y coordinates of all bees found within the nest across all time points), and then averaging each bee's distance from that center over frames where they were detected. (6) We calculated degree centrality, or the number of unique bees that each bee interacted with, using the igraph package in R(*41*). Bees were considered to have interacted if their tags were located within 1 cm of each other at any point during the recording (see above for validation of this spatial threshold for physical contact).

Bees that had a low detection frequency (i.e., were found in less than 250 seconds out of 3600 seconds of video) were removed from network analyses to avoid unreliable estimates of interaction frequency, although this affected only a small portion of the dataset (20 out of 310 bees) and did not qualitatively affect any results.

For all variables, we calculated each bee's change from before to after treatment. For instance, if a bee moved more slowly after treatment as compared to before, the change in its average speed would be negative.

We performed multivariate multiple regression with six dependent variables – change in proportion of time active, change in proportion of time on the nest, change in active speed, change

in distance to the queen, change in distance from the social center, and change in degree centrality. This analysis was appropriate because the in-nest measurements had approximate multivariate normality. We initially included treatment, colony, and body weight as covariates, as well as an interaction term, weight*treatment and colony*treatment. Likelihood ratio tests confirmed that colony*treatment, weight*treatment, and weight did not significantly improve the fit of the model, so our final model included only colony and treatment as independent variables.

We evaluated the assumptions of multivariate multiple regression in several ways. We checked for multivariate outliers by computing Mahalanobis distances using the R package, mvoutlier(*42*). We removed obvious outliers, reran the analysis, and observed no qualitative changes to results; thus we report the final model, including multivariate outliers. We graphically assessed multivariate normality using a Q-Q plot of squared Mahalanobis distances, and found that it was approximately correctly distributed – again, we found that the outliers do not change our results significantly. We found no evidence that the variance-covariance matrices were heterogeneous, using Box's M test for equality of covariance ($p > 0.001$). Since this test is very sensitive, the level of significance for Box's M test should be taken as 0.001(*43*). We acknowledge that data within each hive may not be completely independent – *e.g.,* treated bees may stop performing colony tasks, causing other non-treated bees to change their behavior.

Analysis of foraging behavior

For each bee observed foraging, we automatically quantified its total number of nectar- and pollen-foraging bouts observed based on tag-tracking data. We classified observations as a single bout of foraging if a bee was identified on a feeder without being absent for more than two minutes; if the bee left the foraging area for at least two minutes and returned, this was classified as a new foraging bout. Because almost all bees that foraged visited both the nectar and pollen feeder during the same visit, we combined pollen and nectar foraging bouts. For binary analyses of foraging (e.g., Table S10), workers were considered "foragers" if they were observed performing any foraging activity. We calculated the change in the number of foraging bouts for each individual by subtracting the number of pre-treatment foraging bouts from the number of post-treatment bouts, for all bees who were observed foraging before or after treatment. Though the resulting variable (change in number of foraging bouts) was discrete, we approximated it as a continuous, normal variable for analysis. The discrete variable is not bounded on either end, and it takes on a large range of integers. Furthermore, we evaluated the model for the assumptions of linearity, normality, equal variance, and no overly-influential outliers. We found no strong evidence that these assumptions were violated. We used a linear model with change in the number of foraging bouts as the dependent variable, and we included colony and treatment as independent variables.

In addition, we used two logistic regressions to determine if the imidacloprid treatment predicted whether bees would either cease foraging or begin foraging after treatment. For the regression predicting whether bees would begin foraging after treatment, we excluded all bees that were observed foraging prior to treatment. For the regression predicting whether bees were likely to cease foraging, we included only bees that were observed foraging prior to treatment. Since the number of new bees that foraged after treatment was very small, we re-analyzed the data with bias-reduced logistic regression(*44*). We investigated a treatment by colony interaction and found no significant improvement in the bias-reduced model. We therefore report the results of the bias-reduced model with no interaction terms for this analysis.

Field thermoregulation experiments

18 queenright commercial bumblebee (*Bombus impatiens*) colonies (BioBest®) (average: 44.0 (s.d. = 11.0) workers, estimated from photos) were deployed at the Concord Field Station in Bedford MA between July 25th and Aug 29th, 2017, in three cohorts of six colonies. In each cohort, three colonies each were randomly assigned to control and treatment (6 ppb imidacloprid, prepared using the same solution preparation protocols described above, but transferring 84 µL concentrated imidacloprid solution into 1400 µL Biogluc® to achieve final desired concentrations, see "*Imidacloprid solution preparation and confirmation*" above) groups. Colonies were given ad libitum access to nectar (either control or treated) 1-2 hours before colonies were placed in the field and colony exit/entrance holes were opened, giving foragers access to the outside environment. No pollen was supplied to colonies after release to encourage natural foraging behavior.

Each colony was outfitted with three waterproof digital temperature probes (DS18B20). Two were placed in direct physical contact with different parts of the developing brood structure within the nest (Fig 3B), and one was suspended in the air within the nest box. Two temperature probes (placed at either end of the 6-colony array) recorded outdoor temperatures. A last temperature probe was placed in either the outdoor air (cohort 1) or dead brood structure (cohorts 2-3) of an empty colony box containing no bees. Data from all 21 temperature probes were recorded roughly every 20 seconds using custom scripts on an Arduino Mega microcontroller for between 9 and 19 days. Data from the two brood temperature probes were averaged at every timestep to yield a mean brood temperature for each colony. Outdoor temperatures were divided into rising and falling periods using a local smoothing window of 3 hours. Because the individual tracking used for other experiments (and described above) requires sensitive electronic equipment not suitable for outdoor use, individual tracking within the nest was not performed for these outdoor thermoregulation experiments.

We analyzed differences in brood temperature between control and treated colonies first by using permutation tests, comparing ability to thermoregulate between treatments (Table S5). We estimated ability to thermoregulate as follows: For each colony, we calculated the average difference between outdoor temperature and colony temperature ("thermoregulation capacity"). We then estimated the difference in thermoregulation capacity between the two treatments (Table S13).

We investigated other trends in thermoregulation ability using General Additive Mixed Models (GAMM) that modeled brood and air temperature as response variables, outdoor temperature, treatment, time of day, and rising/falling temperature periods as fixed effects, and experimental day number and colony as random effects (Tables S6). We found no evidence that including random slopes that allowed colonies to differ in their response to treatment significantly improved the models, so we used random intercepts only. We used a random subsample of 20,000 data points from a total possible 140,531 to allow GAMMs to run in a reasonable amount of time. We found that adding cohort to the model improved predictive power only for the model for air temperature inside the hive, but not for the model for brood temperature. We therefore removed the cohort predictor from the brood temperature model. For the GAMMs, we set the smoothing parameter, 'k' to 5, to try to avoid overfitting and to allow models to run in a reasonable amount of time(*45*). We used AIC to evaluate which predictors to include in our final models.

Presence of insulating wax canopy (either partial or complete) was scored for each colony from photos taken every 4-5 days, including the beginning and end of each experiment. Scores at the end of each experiment were used to test for differences between treatment (Fig 3F), but all colonies that constructed wax canopies by the end of the experiment had initiated at least partial construction by the end of the experiment's first week, so the difference in experimental timescales for different colonies had no effect on results. No colonies had either a partial or complete wax canopy at the beginning of the experiment. All photos were scored by two independent observers, one blinded and one knowledgeable about hypotheses and treatment schema, which resulted in identical scores.

Supplementary online text

Agent-based modeling

We created a computational model called the bee nest agent-based model (BeeNestABM(*46*), available at https://github.com/ashleefv/BeeNestABM) to simulate the movements of individuals bees within a nest chamber, taking into account interactions with nestmates and nest structures. The model consists of a series of steps that define how the bees move and/or interact at each time step (0.5 s): (1) calculate the distances between each pair of bees and the distances between each bee and each nest structure object, (2) probabilistically transition each bee among active and inactive states, and (3) move each active bee with some speed and at some heading. The bees are allowed to transition between active and inactive states both spontaneously and due to social influences if they come within a 1 cm (approximately one body length) of another bee. All models were populated with empirical data on (a) numbers of bees and (b) brood and nest locations from a single acute-exposure colony.

We empirically estimated the probability of transitioning between the states spontaneously and under social influence from observations of bee colonies over the course of one hour. We first measured the rates (i.e., Markov transition probabilities) of active (i.e., mobile) bees becoming inactive ($p_{A\rightarrow I}$) and vice-versa ($p_{I\rightarrow A}$, Fig S4). These rates were measured separately depending on physical contact with nestmates and when bees were located on or off the nest structure (Fig S4). In untreated colonies (i.e., pre-exposure), workers were more likely both to become active after being inactive (higher $p_{I\rightarrow A}$) or to remain active when already active (lower $p_{A\rightarrow I}$) immediately after physical contact with a nestmate, independent of spatial location (i.e. on vs. off the nest structure, all $p < 0.05$). When located off the nest structure, workers fed 1.0 ng imidacloprid were less likely to become active when inactive ($p_{I\rightarrow A}$) and more likely to become inactive when active ($p_{A\rightarrow I}$) than controls, both spontaneously and after physical contact with a nestmate (Fig S5). In contrast, imidacloprid exposure had relatively weak effects on activity when bees were on the nest structure, where bees are generally more crowded and mobile (Fig S5). Reduced sensitivity to physical contact could result from imidacloprid's direct effects on cholinergic mechanosensory neurons(*47*). These eight empirical worker mobility transition rates ($p_{A\rightarrow I}$ and $p_{I\rightarrow A}$, depending on location and social contact, Figs S4-5) were used to model worker mobility state.

In our model, the speed of individual active bees is independently sampled from a distribution of realistic bee speeds observed in four colonies over 1 hour without pesticide exposure. Bee movements were physically bounded within a 25 x 20 cm range, approximately replicating the physical dimensions of the nest during acute exposure trials (Fig S4). Movements

outside of this range were constrained along the "wall" and speed was adjusted using the component of their movement vector that was parallel to the "wall" (Fig S4).

The angle of motion for each active bee is determined by a random walk with a bias toward the nest center (μ) determining the relative weights of a random walk ($\hat{v}_{rw}$, drawn from a uniform distribution at each frame constrained within +/- 45 degrees of the current angle heading) and angle to the nest center ($\hat{v}_{nest}$, Fig S4). The strength of this bias (μ) for pre-exposure untreated bees and post exposure high dose treated bees were determined by parameter estimation where the weights in the model were varied to fit the simulation results to empirical observations. The fitting was conducted in MATLAB using the fmincon optimization function to minimize the weighted sum of squared differences between the BeeNestABM simulation results for metrics averaged over the entire bee nest population over 1 hour and the empirical data from the same colony for pre- and post-exposure cases (Fig S12). To determine the overall fit score, the least squares residuals of these metrics were weighted by the inverse of their variance. The metrics used for the parameter estimation and assessing the simulation results and empirical observations are: activity, distance to nestmates, mean distance to nest structures, mean distance to the center of the nest, the portion of time on nest, and the rate of interaction with nestmates, all taken as group means.

We implemented two model variants to independently evaluate independent impacts of 1.0 ng imidacloprid exposure on activity parameters and attraction to the nest center. To test the hypothesis that the observed nest behavior effects of imidacloprid could be attributed to effects on the activity of treated bees, we implemented an "activity-only" model variant (Fig S6). In this model, movement of "treated" workers (i.e., 28 out of 111 bees, matching the number of bees experimentally fed 1.0 ng imidacloprid in colony 1) within the nest was simulated using activity parameters ($p_{A\rightarrow I}$ and $p_{I\rightarrow A}$) derived from bees exposed to 1.0 ng imidacloprid. Activity parameters were randomly sampled (with replacement) from the set of individually-estimated parameters derived from treated workers. Activity of "control" workers was simulated identically, but by sampling parameters from "control" bees, fed 0 ng imidacloprid (while holding attraction to the nest structure, μ, for "treated" bees equivalent to controls).

To test the alternative hypothesis that the nest behavior effects of imidacloprid are attributable to imidacloprid's effects on attraction to nest structures, we implemented an "attraction-only" model variant (Fig S6). In this model, treated bees were given the reduced nest attraction (μ) values estimated for bees fed 1.0 ng imidacloprid, but all mobility parameters were matched to controls. In the "full" model variant, all imidacloprid-specific parameters (p and μ) were included in the model. Each model variant was run for 1000 iterations, with 7200 timesteps (equivalent to empirical trials of 1 hour of data collected at 2 Hz).

These models disentangle the effects of imidacloprid on activity and space-use within bumblebee nests. Bees simulated with "treated" activity parameters ($p_{A\rightarrow I}$ and $p_{I\rightarrow A}$) but "control" nest attraction parameters (μ) exhibited reduced time on the nest structure, reduced interaction rates, and increased distance from the nest center, in addition to direct effects on activity (Fig S6). This demonstrates that direct effects on activity may yield secondary effects on spatial distribution, nursing, and interaction rates.

However, changing activity parameters alone did not fully recapitulate the behavioral effects of imidacloprid treatment; bees simulated with imidacloprid's effects on both activity and nest attraction parameters exhibited even greater reductions in time on nest, interaction rates and proximity to the nest center ("full" models, Fig S6). Overall, this analysis suggests that the direct effects of imidacloprid on activity (and its modulation by contact with nestmates) and the

strength of attraction to the nest structure combine to drive the observed effects of imidacloprid exposure on nest behavior.

Rationale for dosages and concentrations

Neonicotinoids and their metabolites are regularly found in plant tissues, including nectar and pollen(*7*, *48*). When applied to the soil, imidacloprid can be incorporated into nectar for up to ~230 days after application(*49*). A recent review(*48*) found typical environmental concentrations of neonicotinoids in pesticides to be between 2-6 ng/g, but the amount of imidacloprid found in pollen and nectar varies, with measurements of 10 ppb in nectar and 14 ppb in pollen from squash(*50*), 16 ppb in nectar of buckwheat(*51*), and 12.8 ppb in nectar of citrus trees(*49*). In the citrus experiment, Byrne et al.(*49*) found that when imidacloprid was applied at the full, manufacturer-recommended rate, the highest reported value in nectar was 21.9 ppb; however, taking into account the total residues of imidacloprid plus its metabolites, the highest amount reported was 37.1 ppb. Furthermore, the highest amount of total residues in uncapped nectar from the hive comb of nearby honeybees was found to be 95.2 ppb (*49*). In addition to neonicotinoid exposure via crops, contaminated wildflowers (for example growing on field margins) also represent a significant route of neonicotinoid exposure(*52*, *53*), with neonicotinoid concentrations that can exceed levels in crops themselves. For example, pollen collected from oilseed rape flowers contained a mean concentration of 3.26 ng/g of thiamethoxam (range: 1.02-11.10), while pollen collected from wildflowers growing on oilseed rape field margins had a mean concentration of 14.81 ng/g (range: <0.12 – 86.02)(*53*)

While there is disagreement on the reversibility of the effects of neonicotinoids, some studies have suggested that honeybees and bumblebees can clear non-lethal doses of imidacloprid from their bodies – with honeybees clearing 2 ng per day, and bumblebees clearing 7 ng per day(*39*).

Studies disagree about whether a single, concentrated dose or a chronic, low dose of imidacloprid is more harmful to bees. Cresswell et al.(*39*) suggest that an acute, concentrated dose would have a larger deleterious effect on bees, while Suchail et al.(*54*) claimed that chronic exposure to honeybees was toxic at a dose that was 60-6000 times lower than the acute dose required to produce the same effect.

Experiments involving chronic exposure (i.e., ad libitum access to contaminated nectar) may more accurately mimic field-realistic conditions that bumblebees experience, but measuring the exact amount of pesticide ingested is difficult in these studies. The choice of 1ng of imidacloprid as a high-treatment dose in the acute experiments closely matches the average amount of imidacloprid that bumblebees consumed each day during the chronic pesticide experiment; overall mean nectar consumption was 201 mg/day per bee (which did not differ between treatments, Control v imidacloprid, $W = 29$, $p = 0.34$, Mann-Whitney U test), which at an imidacloprid concentration of 4.7 ng/g (6 ppb imidacloprid in nectar solution weighing 1.272 g/mL) would result in a mean daily consumption of 0.95 ng imidacloprid per bee.

Supplementary Figures:

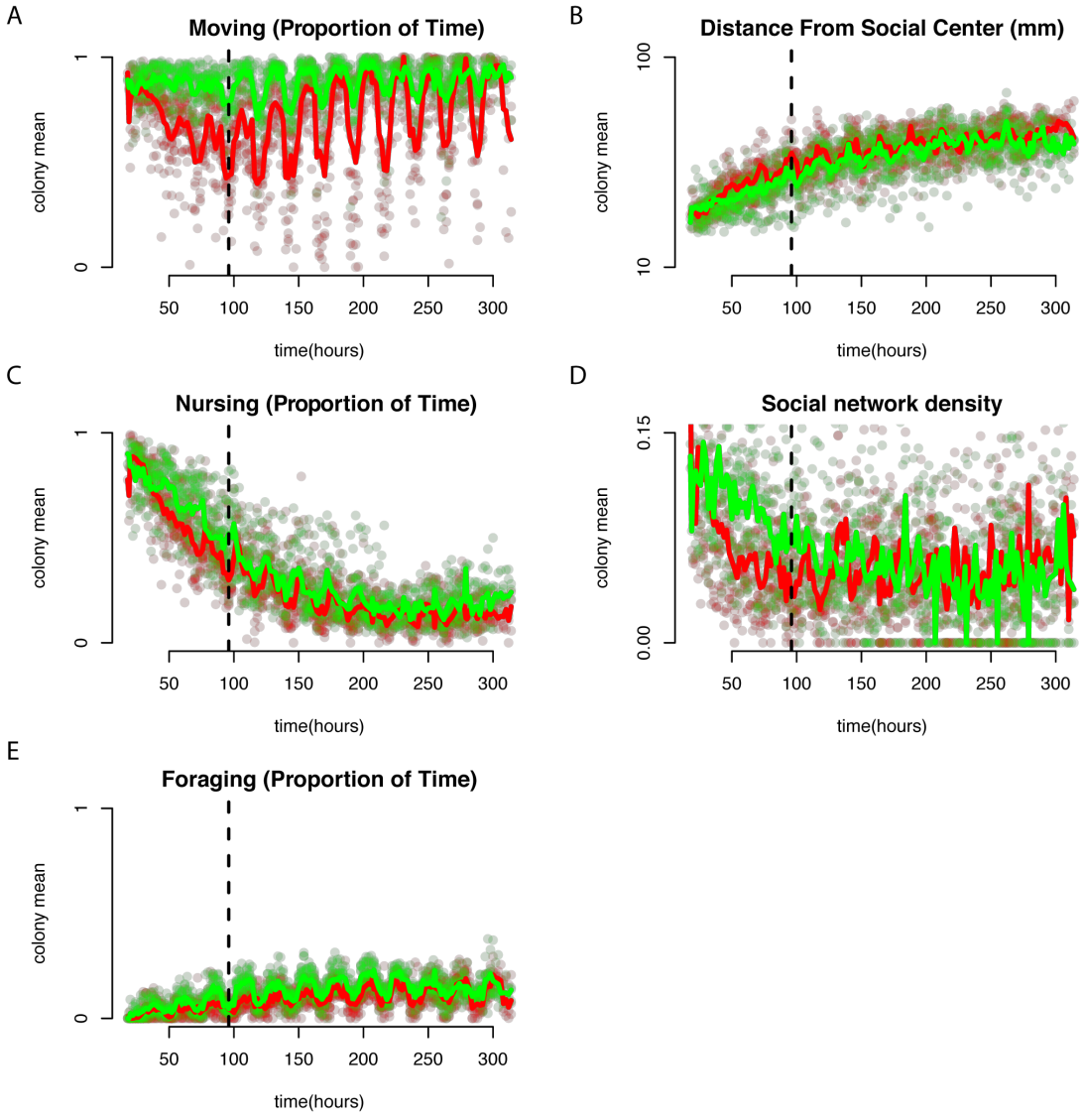

Figure S1. Colony average behavioral metrics for the full time-course of experiments. Colony mean (A) activity, (B) distance form center, (C) nursing, (D) social network density, and (E) foraging activity across time for imidacloprid-exposed colonies (red) and control colonies (green). Transparent filled markers show single colony averages, and solid lines show average across all colonies within different treatment groups. Vertical dashed line shows a cutoff of the first 4 days of the experiment, used as an acclimation cutoff for data in Figure S2. Effect sizes for these data are reported in Figure S2.

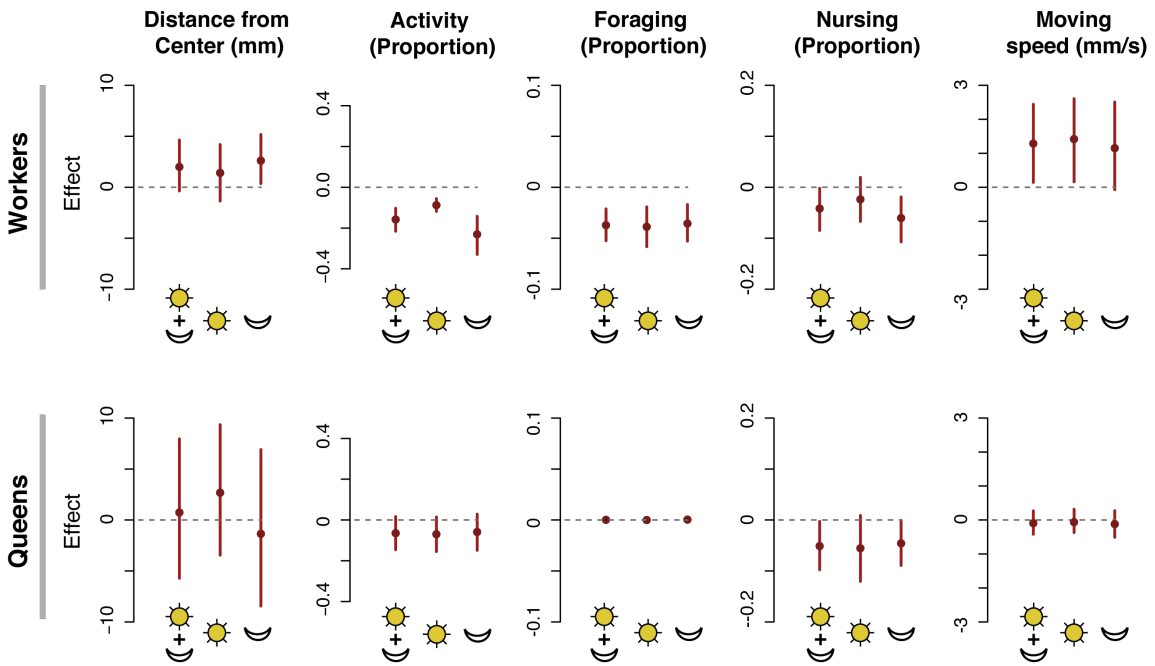

Figure S2. Effect plots for all behavioral metrics by time of day, experimental period, and reproductive caste. For each metric, open circles show the mean effect size and vertical lines show the 95% CI based on 10000 hierarchical bootstrap replicates. Within each panel, CIs are shown separately for runs when all time periods are pooled (left), or when night (middle) and day (right) periods are analyzed separately. Data from workers and queens analyzed separately is shown on the top and bottom, respectively. See datasets and figures at zenodo.org *(32)* for further analyses, including changes in effects over time.

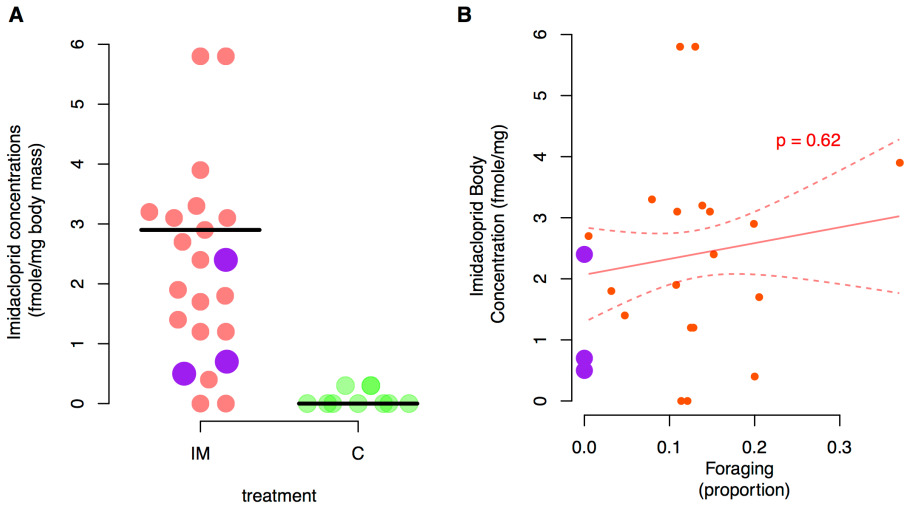

Figure S3. Imidacloprid body concentration. (A) Imidacloprid body concentrations by treatment group. Filled circles show concentrations from individual bees (small red markers for workers, larger purple markers for queens), and black lines show median values for each group (C v IM, W = 207, p = 7.2 x 10^{-5}, Mann-Whitney U test). (B) Imidacloprid body concentrations v. foraging activity (proportion of time in proximity to feeder). Small red markers and large purple markers show results for workers and queens, respectively. Dotted lines in (B) represent the 95% CI of the regression line (solid line).

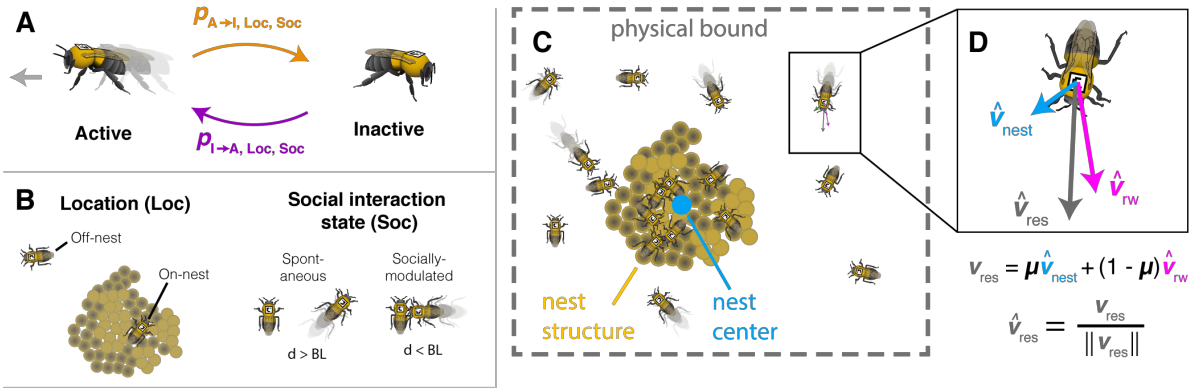

Figure S4. Agent-based modeling of *B. impatiens* nest behavior. (A-B) Empirical estimation of Markov mobility state-switching model. (A) Schematic of Markov mobility state-switching probabilities (active to inactive and vice-versa) based on location and social-interaction state. (B) Schematics illustrating contexts (Loc and Soc) that modulate worker transitions between active and inactive states. (A) Schematic diagram of the elements of an agent-based model of worker movement within the nest. (B) Schematic illustrating how realistic worker random locomotion was simulated. On a frame-by-frame basis, the resultant direction of worker motion ($\hat{v}_{res}$) was determined by the weighted (μ) summing of a random walk vector ($\hat{v}_{rw}$) and a vector of attraction back to the nest center ($\hat{v}_{nest}$). (A) Schematic diagram of the elements of an agent-based model of worker movement within the nest. (B) Schematic illustrating how realistic worker random locomotion was simulated. On a frame-by-frame basis, the resultant direction of worker motion ($\hat{v}_{res}$) was determined by the weighted (μ) summing of a random walk vector ($\hat{v}_{rw}$) and a vector of attraction back to the nest center ($\hat{v}_{nest}$).

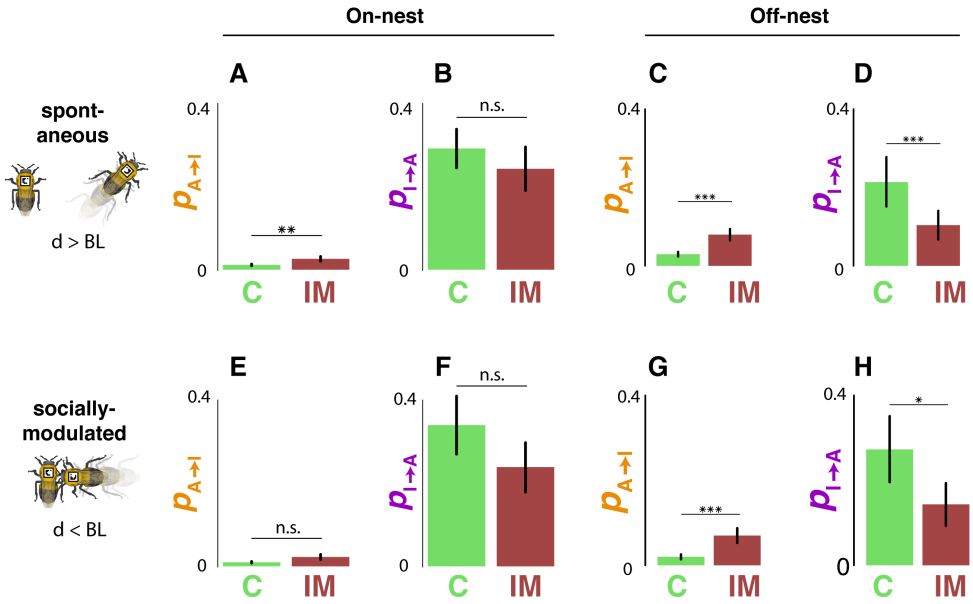

Figure S5. Effects of acute imidacloprid exposure on mobility switching parameters. $p_{A\to I}$ and $p_{I\to A}$ estimates for bees fed 1.0 ng imidacloprid (1.0 ng) and control bees (C), shown separately depending on social-interaction state (spontaneous, or social-modulated) and location (on or off the nest structure). For each, bar plots show the mean estimate and 95% bootstrap confidence intervals (black lines) for bees fed control sucrose solution (C) and bees fed 1.0 ng imidacloprid (IM). *, **, and *** indicate p < 0.05, .005, and 0.005 (respectively) by Wilcoxon signed-rank test.

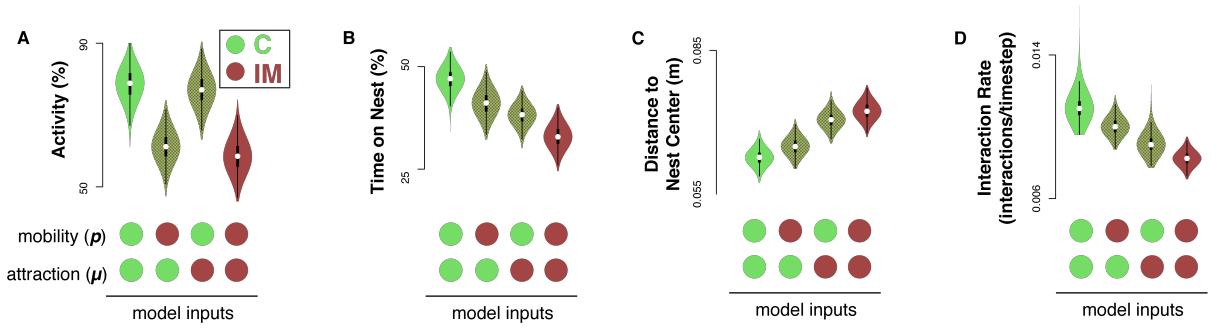

Figure S6. Effects of model inputs on simulated worker behavior. Simulated (A) activity, (B) portion of time on nest structure, (C) distance to the nest center, and (D) interaction rate, and under different simulated conditions. For each, "control", "activity", "attraction", and "full" models are shown from left to right (see Materials and Methods), with solid fill markers below each panel showing whether parameter estimates for control (C, green) or imidacloprid-treated bees (IM, red, data from bees fed 1.0 ng imidacloprid) were used as model inputs for mobility (p) and attraction (μ) parameters. White dots show the median and violin plots show the estimated distribution of trial means (for the group of "treated" bees, or ~1/3 of the colony) across 1000 simulations.

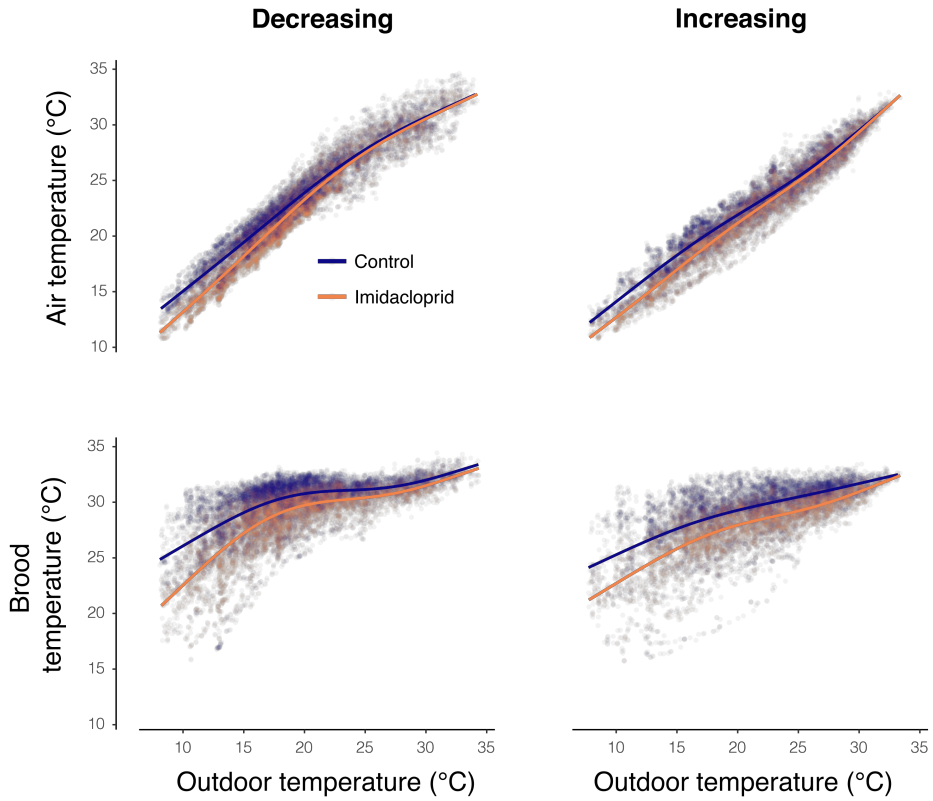

Figure S7. Smoothed estimates of outdoor temperature vs colony temperature show that imidacloprid-treated colonies' temperature regulation ability decreases as outdoor temperature decreases. Rows show different measurements of temperature (Brood and Air), and columns show subsets of data for times of day when temperature was either increasing or decreasing. Lines show predicted means, based on a Generalized Additive Model (based on a subsample of 50,000 data points) that includes temperature direction, measurement location, and treatment. A separate smooth was fit for time of day and outdoor temperature for each level of the interaction between treatment and temperature direction -- 1) Control group, temp decreasing, 2) Control group, temp increasing, 3) Treatment group, temp decreasing, and 4) treatment group, temp increasing. There are significant interactions between treatment and increasing/decreasing temperature for both air and brood temperature (model results described in Tables S14-15).

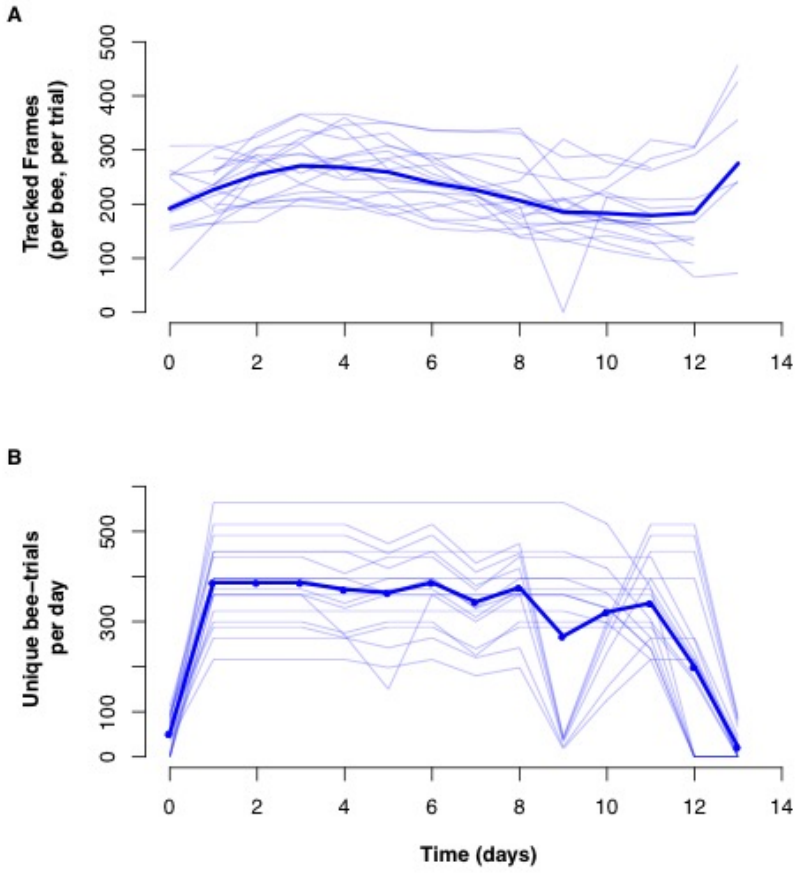

Figure S8. Tracking performance over time. (a) Mean frames tracked per video trial per tracked bee and (b) Mean total number of unique trials (including multiple trials from the same individual) over the experimental period. In each, thin lines show trends for individual colonies, and thick lines show mean trends across all colonies. The reduction in bee-trials per day (panel B) on day 9 resulted from temporary computer failure for one experimental cohort (six colonies). Decreases unique trials on days 0 and 13 result from partial days of tracking.

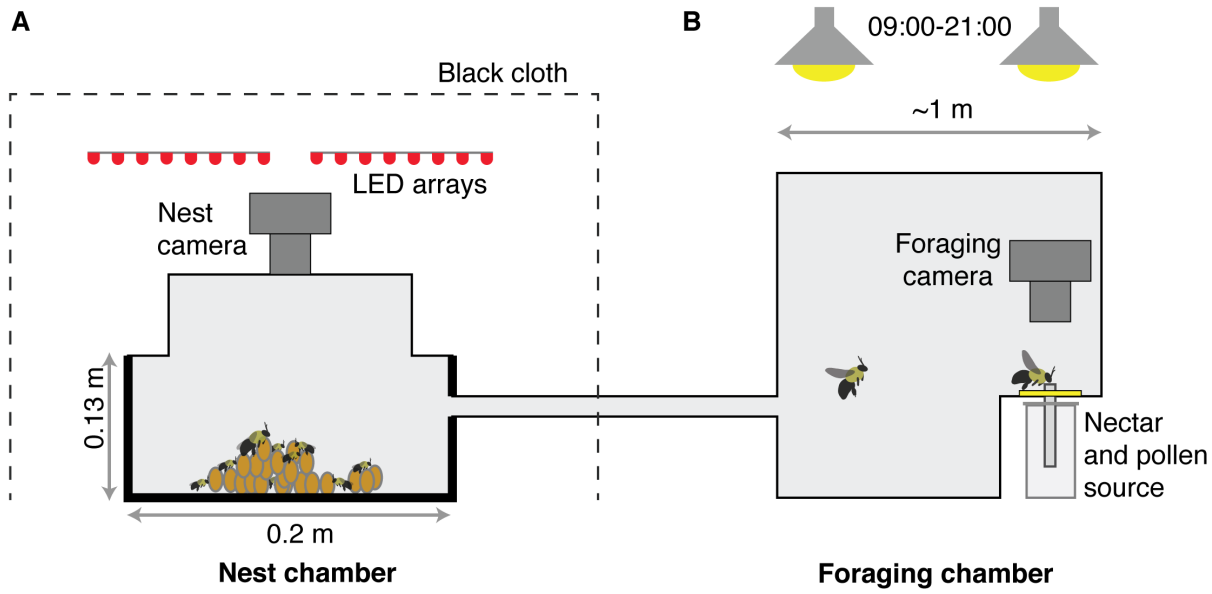

Figure S9. Schematic of acute exposure experimental tracking arena. (A) Nest chamber. Thick black lines show opaque, black plastic nest box, and thin lines show transparent plastic cover. Dotted line indicated black drop cloth draped over nest chamber and cameras. (B) Foraging chamber, showing relative positions of lights, foraging camera, and nectar and pollen source. Drawing is not to scale.

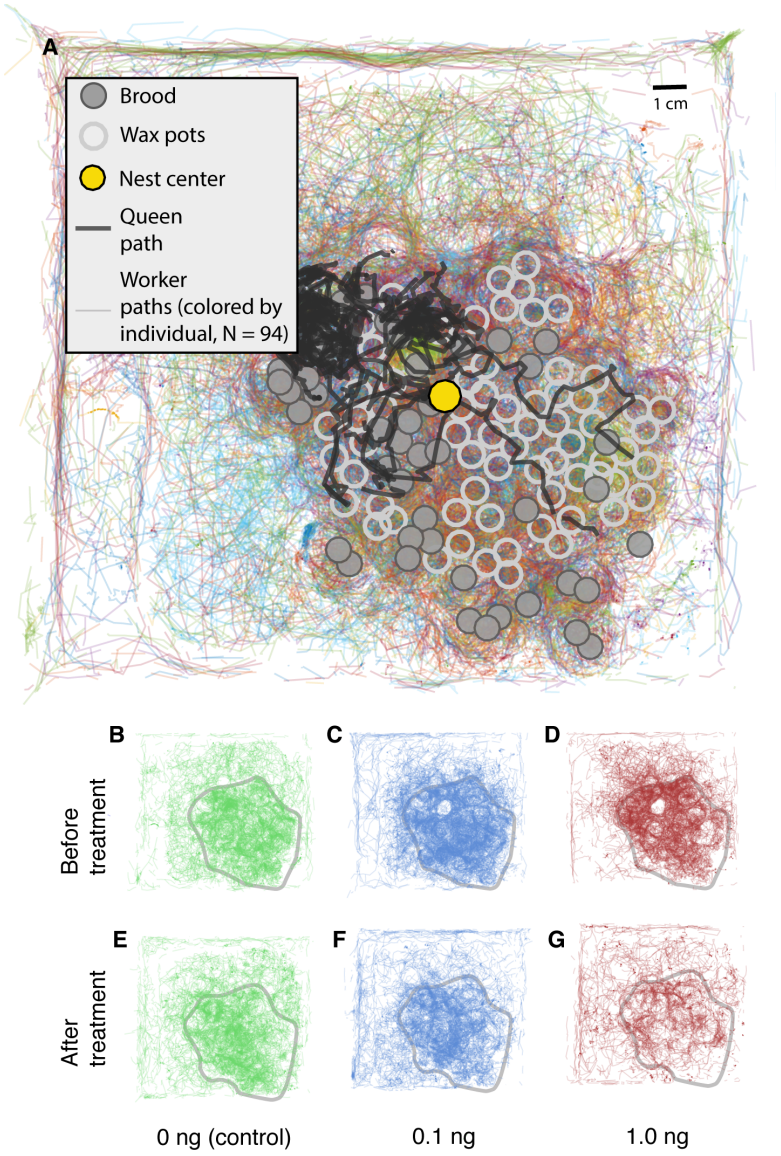

Figure S10. Example path-tracking within *Bombus impatiens* nests. (A) Mapping of individual movement patterns and relevant nest elements from a single colony from acute exposure trials. Thin, transparent lines represent the paths of individual workers (N = 94, each identified with a unique color) within the nest over the course of an hour. Filled gray circles indicate positions of developing brood (eggs, larvae, and pupae), while empty gray circle represent the position of honeypots. Thick black line represents the path of the queen and the large yellow circle shows the position of the social center of the colony. (B-G) Tracked positions of control (B: 0 ng) and imidacloprid-fed (C: 0.1 ng and D: 1.0 ng) bees during an hour of observation 24 hours before treatment. (E-G) Tracked positions of the same control (F) and imidacloprid-fed bees (G-H) 24 hours after treatment. In (B-G), nest structures (i.e., wax pots and developing brood) are outlined in gray.

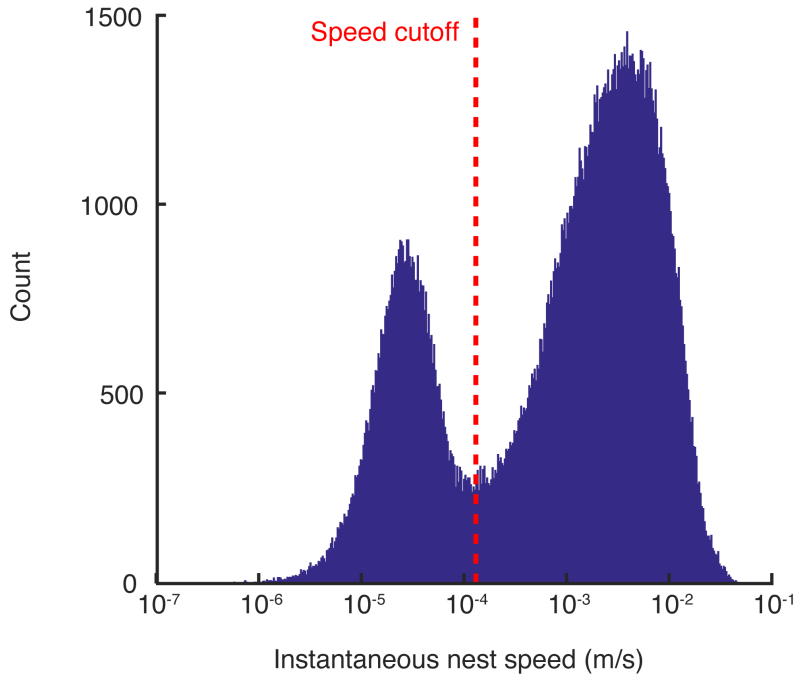

Figure S11. Histogram of all instantaneous measured speeds (N = 197,981) for all individuals within Colony A before treatment over an hour of observation. Dotted red line indicates the speed cutoff used throughout. Instantaneous speeds below this cutoff (0.13 mm/s) were assumed to result from digital noise, rather than real movements of bees.

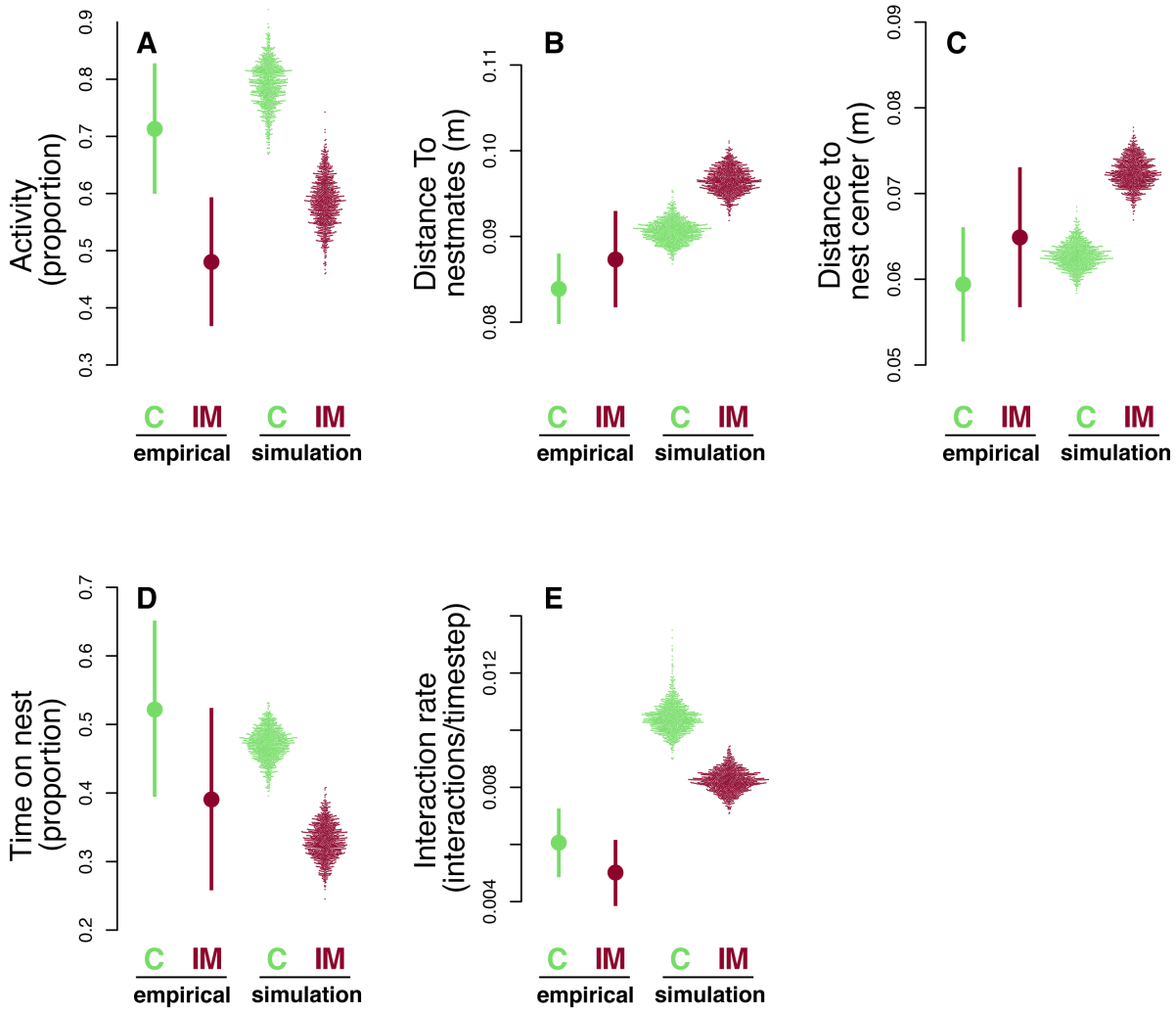

Figure S12. **Comparison of agent-based simulation output and empirical data.** (A) Activity, (B) distance to nestmates, (C) distance to the nest center, (D) portion of time on the nest structure, and (E) interaction rate. For each metric, empirical results (for the colony used for model optimization) are shown on the left, with solid markers showing the mean and 95% bootstrap CI, and simulated results are shown on the right, with beeswarm plots showing the distribution of group means across 1000 replicate simulations (each represented by a separate marker). For each, control (i.e., untreated) bees are shown on the left ("C", green), and "treated" bees are shown on the right ("IM", red).

Supplementary Tables:

Table S1. **Type II MANOVA, using Pillai test statistic, for overall model for change in six dependent variables (portion of time active, portion of time on nest, active speed, queen distance, social distance, and degree centrality) and two independent variables (imidacloprid treatment and colony).** Data from acute imidacloprid experiments.

	df	test stat	Approx F	num df	den df	p-value
Imidacloprid treatment	2	0.36	9.07	12	490	7.66×10^{-16}
Colony	3	0.22	3.24	18	738	6.44×10^{-6}

Table S2. Summary of regressions for acute imidacloprid experiments. Within each summary, we show regression using treatment contrasts with reference levels = 0 ng imidacloprid and Colony A. At the bottom row of each summary, we show regression coefficient for differences in 0.1 and 1 ng imidacloprid groups calculated by changing the reference level for imidacloprid to 0.1 ng imidacloprid.

Summary of regression for change in portion of time active as a function of imidacloprid treatment and colony (F(5, 249) = 26.14; p-value < 2.2 × 10^-16)		**Estimate**	**Std. Error**	**t-value**	**p-value**
	(Intercept)	-0.097	0.04	-2.42	0.016
	Imidacloprid: 0 ng group - 0.1 ng group	-0.0305	0.039	-0.77	0.44
	Imidacloprid: 0 ng group - 1 ng group	-0.384	0.039	-9.8	< 2 × 10^-16
	Colony A - B	0.154	0.045	3.44	6.8 ×10^-4
	Colony A - C	0.111	0.049	2.25	0.025
	Colony A - D	0.024	0.043	0.56	0.573
	Imidacloprid: 0.1 ng group - 1 ng group	-0.354	0.0394	-8.97	< 2 ×10^-16
Summary of regression for change in portion of time on nest as a function of imidacloprid treatment and colony (F(5, 249) = 7.266; p-value = 2.262 × 10^-6).		**Estimate**	**Std. Error**	**t-value**	**p-value**
	(Intercept)	-0.1	0.055	-1.81	0.071
	Imidacloprid: 0 ng group - 0.1 ng group	0.006	0.055	0.11	0.915
	Imidacloprid: 0 ng group - 1 ng group	-0.261	0.055	-4.78	3.03 × 10^-6
	Colony A - B	0.138	0.062	2.2	0.029
	Colony A - C	0.051	0.069	0.74	0.458

	Colony A - D	0.089	0.06	1.49	0.137
	Imidacloprid: 0.1 ng group - 1 ng group	-0.267	0.055	-4.86	2.08 ×10^-6
Summary of regression for change active speed as a function of imidacloprid treatment and colony (F(5, 249) = 4.992; p-value = 0.00022)		**Estimate (m/s)**	**Std. Error**	**t-value**	**p-value**
	(Intercept)	-0.000029	0.000282	-0.1	0.92
	Imidacloprid: 0 ng group - 0.1 ng group	0.000024	0.000279	0.09	0.932
	Imidacloprid: 0 ng group - 1 ng group	-0.001126	0.000277	-4.06	6.61 × 10^-5
	Colony A - B	0.000121	0.000317	0.38	0.703
	Colony A - C	-0.000014	0.000349	-0.04	0.968
	Colony A - D	-0.000398	0.000304	-1.31	0.192
	Imidacloprid: 0.1 ng group - 1 ng group	-0.00115	0.000279	-4.12	5.11 × 10^-5
Summary of regression for change social distance (distance from nest center) as a function of imidacloprid treatment and colony (F(5, 249) = 5.304; p-value = 0.00012).		**Estimate (m)**	**Std. Error**	**t-value**	**p-value**
	(Intercept)	0.0033	0.0032	1.05	0.294
	Imidacloprid: 0 ng group - 0.1 ng group	0.0012	0.0031	0.37	0.71
	Imidacloprid: 0 ng group - 1 ng group	0.0127	0.0031	4.08	5.99 × 10^-5
	Colony A - B	-0.0045	0.0036	-1.27	0.207
	Colony A - C	0.0019	0.0039	0.49	0.623
	Colony A - D	-0.0051	0.0034	-1.48	0.14
	Imidacloprid: 0.1 ng group - 1 ng group	0.01158	0.0031	3.69	2.76 × 10^-4
Summary of regression for change distance from queen as a function of imidacloprid treatment and colony		**Estimate (m)**	**Std. Error**	**t value**	**p-value**
	(Intercept)	0.0034	0.0038	0.89	0.374
	Imidacloprid: 0 ng group - 0.1 ng group	-0.0018	0.0038	-0.46	0.645

(F(5, 249) = 6.36; p-value = 1.406 × 10^-5)	Imidacloprid: 0 ng group - 1 ng group	0.014	0.0038	3.69	2.80 × 10^-4
	Colony A - B	-0.0083	0.0043	-1.91	0.057
	Colony A - C	0.0058	0.0048	1.22	0.222
	Colony A - D	-0.005	0.0042	-1.19	0.235
	Imidacloprid: 0.1 ng group - 1 ng group	0.0157	0.0038	4.13	5.03 × 10^-5
Summary of regression for change degree centrality as a function of imidacloprid treatment and colony (F(5, 249) = 11.61; p-value = 4.308 × 10^-10).		**Estimate**	**Std. Error**	**t-value**	**p-value**
	(Intercept)	-17.5	2.2	-7.95	6.64 × 10-14
	Imidacloprid: 0 ng group - 0.1 ng group	0.9	2.17	0.4	0.688
	Imidacloprid: 0 ng group - 1 ng group	-10.6	2.17	-4.91	1.68 × 10-6
	Colony A - B	10	2.48	4.06	6.68 × 10-5
	Colony A - C	-1	2.72	-0.36	0.719
	Colony A - D	1.7	2.38	0.73	0.465
	Imidacloprid: 0.1 ng group - 1 ng group	-11.5	2.18	-5.28	2.80 × 10-7
Summary of regression for change in number of foraging bouts as a function of imidacloprid treatment and colony (F(5, 117) = 4.931; p-value = 0.00039).		**Estimate (count)**	**Std. Error**	**t-value**	**p-value**
	(Intercept)	5.5	4	1.37	0.173
	Imidacloprid: 0 ng group - 0.1 ng group	-5.4	3.6	-1.49	0.139
	Imidacloprid: 0 ng group - 1 ng group	-13.9	3.9	-3.57	5.13 × 10^-4
	Colony A - B	-3.3	4.6	-0.71	0.478
	Colony A - C	8.9	4.4	2.03	0.045
	Colony A - D	2.2	4.8	0.46	0.65
	Imidacloprid: 0.1 ng group - 1 ng group	-8.6	3.9	-2.18	0.032
Summary of bias-reduced logistic		**Estimate (log odds**	**Std. Error**	**Chisq**	**p-value**

regression for becoming a new forager as a function of imidacloprid treatment (χ(2)2 = 11.15; p-value = 0.0037).		**of being a new forager)**			
	(Intercept)	-1.7	0.31	40.5	1.95 × 10^-10
	Imidacloprid: 0 ng group - 0.1 ng group	-0.14	0.46	0.1	0.751
	Imidacloprid: 0 ng group - 1 ng group	-2.21	0.88	9.97	0.0016
	Imidacloprid: 0.1 ng group - 1 ng group	-2.06	0.9	8.05	0.0045
Summary of logistic regression for ceasing foraging as a function of imidacloprid treatment (χ(2)2 = 2.2607; p-value = 0.32). Colony and colony by treatment interaction were removed from the regression because it did not significantly improve the model fit. The model includes only bees that foraged prior to treatment with imidacloprid (n = 100).		**Estimate (log odds of ceasing to forage)**	**Std. Error**	**z-value**	**p-value**
	(Intercept)	-1.14	0.41	-2.81	0.005
	Imidacloprid: 0 ng group - 0.1 ng group	-0.21	0.59	-0.36	0.72
	Imidacloprid: 0 ng group - 1 ng group	0.58	0.54	1.07	0.287
	Imidacloprid: 0.1 ng group - 1 ng group	0.79	0.56	1.42	0.156

716
717
718

Table S3. Counts of individuals that foraged after treatment but not before treatment (stratified by imidacloprid treatment). Data from acute imidacloprid experiments.

Imidacloprid dose	0 ng	0.1 ng	1 ng
Number of new foragers	12	10	1
Total possible new foragers	78	74	73

Table S4. Counts of foragers that ceased foraging for each imidacloprid treatment group. Data from acute imidacloprid experiments.

	0 ng	0.1 ng	1 ng
Number of foragers that ceased foraging after treatment	8	7	12
Total number of foragers before treatment	33	34	33

Table S5. Differences in ability of colonies to maintain temperatures in field thermoregulation experiments. Estimates = (treatment hive temp – outdoor temp) – (control hive temp – outdoor temp). The interpretation for the estimate of -0.76 is as follows: On average, the colonies that consumed imidacloprid kept the air temperature inside their colonies 0.76 °C lower from outdoor temperature, than colonies that consumed no imidacloprid. The lower and upper 95% bootstrap confidence intervals were calculated from 100,000 bootstrap samples. The p-value was calculated using a permutation test based on mean colony temperatures for 18 colonies (9 treatment and 9 control), with 100,000 samples. We conducted the same analysis for both brood and air temperature measurements.

Location	Estimated difference in thermoregulation ability between treated and un-treated colonies (°C)	Lower CI	Upper CI	Perm test p-value
Air	-0.76	-1.21	-0.27	0.0085
Brood	-1.42	-2.15	-0.57	0.0046

Table S6. (Top) Results from Generalized Additive Mixed effects Model (GAMM) to predict brood temperature. (Bottom) Results from Generalized Additive Mixed effects Model (GAMM) to predict air temperature inside the colonies. The GAMMs have three parts, random effects (not shown), parametric coefficients, and smooth terms. The model below included colony and day of the experiment as random effects. Cohort was not included because it was not found to significantly improve the model. For the parametric part of the model, the reference level (Intercept) is the brood temperature for control group, while the temperature is increasing. The other estimates for parametric coefficients are relative to the reference. For instance, "Group: treatment_grp, Temp: Decreasing" means that the model predicts that the treatment group, while temperature is decreasing is 1.46 degrees lower than the reference level. The smooth terms indicate approximate significance of nonlinear terms. To avoid overfitting, we choose the smoothing parameter, "k" to be 5 – this limits the smooth terms to be less than a 5^{th} degree polynomial. For the smoothed terms, a low p-value roughly means that a nonlinear term makes the model significantly better than if the term was added linearly. The first row of smoothed terms, "s(outdoor), for Group: control_grp, Temp: Decreasing" indicates brood temperature is better predicted by a smooth of outdoor temperature for the control group when temperature is decreasing than by a straight line. These models were built from a subsample of 20,000 data points (from the total 140,531 possible data points), to allow the model to run in a reasonable amount of time.

Parametric coefficients (Brood Temp)	**Estimate (°C)**	**Std. Err.**	**t-value**	**p-value**
(Intercept)	30.01	0.33	89.77	<2x10^-16
Group: treatment_grp, Temp: Decreasing	-1.46	0.45	-3.26	0.0011
Group: control_grp, Temp: Increasing	-0.32	0.07	-4.74	2.1x10^-6
Group: treatment_grp, Temp: Increasing	-1.95	0.45	-4.33	1.52x10^-5

Smooth Terms (Brood Temp)	**Estimated df**	**F**	**Approx. p-value**
s(outdoor), for Group: control_grp, Temp: Decreasing	3.8	453.5	<2x10^-16
s(outdoor), for Group: treatment_grp, Temp: Decreasing	4	1121.2	<2x10^-16
s(outdoor), for Group: control_grp, Temp: Increasing	3.5	383.2	<2x10^-16
s(outdoor):Group: treatment_grp, Temp: Increasing	3.9	640.6	<2x10^-16
s(time), for Group: control_grp, Temp: Decreasing	3.8	16.9	3.78x10^-13
s(time), for Group: treatment_grp Temp: Decreasing	3.9	130.4	<2x10^-16
s(time), for Group: tcontrol_grp, Temp: Increasing	3.9	93.7	<2x10^-16

s(time), for Group: treatment_grp, Temp: Increasing		3.9	49.7	<2x10^-16
Parametric coefficients (Air Temp)	**Estimate (°C)**	**Std. Err.**	**t-value**	**p-value**
(Intercept)	22.77	0.23	98.13	<2x10^-16
Group: treatment_grp, Temp: Decreasing	-0.73	0.2	-3.6	0.0003
Group: control_grp, Temp: Increasing	-0.63	0.04	-16.82	<2x10^-16
Group: treatment_grp, Temp: Increasing	-1.54	0.2	-7.59	3.38x10^-14
Cohort 2	1.01	0.32	3.2	0.0014
Cohort 3	0.48	0.31	1.54	0.1234
Smooth Terms (Air Temp)		**Estimated df**	**F**	**Approx. p-value**
s(outdoor), for Group: control_grp, Temp: Decreasing		3.9	10583.9	<2x10^-16
s(outdoor), for Group: treatment_grp, Temp: Decreasing		3.9	12525.1	<2x10^-16
s(outdoor), for Group: control_grp, Temp: Increasing		3.6	7643.1	<2x10^-16
s(outdoor):Group: treatment_grp, Temp: Increasing		3.8	7965.6	<2x10^-16
s(time), for Group: control_grp, Temp: Decreasing		4	493.3	<2x10^-16
s(time), for Group: treatment_grp Temp: Decreasing		4	758.6	<2x10^-16
s(time), for Group: tcontrol_grp, Temp: Increasing		4	546.3	<2x10^-16
s(time), for Group: treatment_grp, Temp: Increasing		4	421.5	<2x10^-16

Supplementary Movies:

Movie S1. Time-lapse video of collecting video trials using the robotic platform shown in Fig 1A. Video is shown at 720x speed (two hours of real time footage).

Movie S2. Tracking of BEEtags within a *B. impatiens* nest after acute imidacloprid exposure. Colors indicate treatment group, with bees in the control, low dose (0.1 ng/bee), and high dose (1.0 ng/bee) groups shown in green, blue, and red, respectively. Bees shown in grey were not removed from the nest for treatment. Frames were recorded at 2 frames per second (fps); playback is at 15fps.

Movie S3. Tracking of foraging behavior of bumblebee (*B. impatiens*) workers. Time-lapse video shows location and identity (in red for all treatment groups) of foragers visiting a nectar feeder (left) and pollen feeder (right) over the course of 55 minutes.

References and Notes

1. A. M. Klein, B. E. Vaissière, J. H. Cane, I. Steffan-Dewenter, S. A. Cunningham, C. Kremen, T. Tscharntke, Importance of pollinators in changing landscapes for world crops. *Proc. Biol. Sci.* **274**, 303–313 (2007). doi:10.1098/rspb.2006.3721 Medline

2. N. Myers, Environmental services of biodiversity. *Proc. Natl. Acad. Sci. U.S.A.* **93**, 2764–2769 (1996). doi:10.1073/pnas.93.7.2764 Medline

3. G. K. Meffe, The potential consequences of pollinator declines on the conservation of biodiversity and stability of food crop yields. *Conserv. Biol.* **12**, 8–17 (1998).

4. N. Gallai, J.-M. Salles, J. Settele, B. E. Vaissière, Economic valuation of the vulnerability of world agriculture confronted with pollinator decline. *Ecol. Econ.* **68**, 810–821 (2009). doi:10.1016/j.ecolecon.2008.06.014

5. J. Fischer, T. Müller, A.-K. Spatz, U. Greggers, B. Grünewald, R. Menzel, Neonicotinoids interfere with specific components of navigation in honeybees. *PLOS ONE* **9**, e91364 (2014). doi:10.1371/journal.pone.0091364 Medline

6. B. A. Woodcock, J. M. Bullock, R. F. Shore, M. S. Heard, M. G. Pereira, J. Redhead, L. Ridding, H. Dean, D. Sleep, P. Henrys, J. Peyton, S. Hulmes, L. Hulmes, M. Sárospataki, C. Saure, M. Edwards, E. Genersch, S. Knäbe, R. F. Pywell, Country-specific effects of neonicotinoid pesticides on honey bees and wild bees. *Science* **356**, 1393–1395 (2017). doi:10.1126/science.aaa1190 Medline

7. M. Rundlöf, G. K. S. Andersson, R. Bommarco, I. Fries, V. Hederström, L. Herbertsson, O. Jonsson, B. K. Klatt, T. R. Pedersen, J. Yourstone, H. G. Smith, Seed coating with a neonicotinoid insecticide negatively affects wild bees. *Nature* **521**, 77–80 (2015). doi:10.1038/nature14420 Medline

8. P. R. Whitehorn, S. O'Connor, F. L. Wackers, D. Goulson, Neonicotinoid pesticide reduces bumble bee colony growth and queen production. *Science* **336**, 351–352 (2012). doi:10.1126/science.1215025 Medline

9. R. J. Gill, O. Ramos-Rodriguez, N. E. Raine, Combined pesticide exposure severely affects individual- and colony-level traits in bees. *Nature* **491**, 105–108 (2012). doi:10.1038/nature11585 Medline

10. M. Henry, M. Béguin, F. Requier, O. Rollin, J.-F. Odoux, P. Aupinel, J. Aptel, S. Tchamitchian, A. Decourtye, A common pesticide decreases foraging success and survival in honey bees. *Science* **336**, 348–350 (2012). doi:10.1126/science.1215039 Medline

11. D. A. Stanley, K. E. Smith, N. E. Raine, Bumblebee learning and memory is impaired by chronic exposure to a neonicotinoid pesticide. *Sci. Rep.* **5**, 16508 (2015). doi:10.1038/srep16508 Medline

12. K. Tan, W. Chen, S. Dong, X. Liu, Y. Wang, J. C. Nieh, A neonicotinoid impairs olfactory learning in Asian honey bees (*Apis cerana*) exposed as larvae or as adults. *Sci. Rep.* **5**, 10989 (2015). Medline

13. R. J. Gill, N. E. Raine, Chronic impairment of bumblebee natural foraging behaviour induced by sublethal pesticide exposure. *Funct. Ecol.* **28**, 1459–1471 (2014). doi:10.1111/1365-2435.12292

14. H. Feltham, K. Park, D. Goulson, Field realistic doses of pesticide imidacloprid reduce bumblebee pollen foraging efficiency. *Ecotoxicology* **23**, 317–323 (2014). doi:10.1007/s10646-014-1189-7 Medline

15. A. N. Arce, T. I. David, E. L. Randall, A. Ramos Rodrigues, T. J. Colgan, Y. Wurm, R. J. Gill, Impact of controlled neonicotinoid exposure on bumblebees in a realistic field setting. *J. Appl. Ecol.* **54**, 1199–1208 (2016). doi:10.1111/1365-2664.12792

16. D. A. Stanley, A. L. Russell, S. J. Morrison, C. Rogers, N. E. Raine, Investigating the impacts of field-realistic exposure to a neonicotinoid pesticide on bumblebee foraging, homing ability and colony growth. *J. Appl. Ecol.* **53**, 1440–1449 (2016). doi:10.1111/1365-2664.12689 Medline

17. E. A. D. Mitchell, B. Mulhauser, M. Mulot, A. Mutabazi, G. Glauser, A. Aebi, A worldwide survey of neonicotinoids in honey. *Science* **358**, 109–111 (2017). doi:10.1126/science.aan3684 Medline

18. S. Tosi, F. J. Démares, S. W. Nicolson, P. Medrzycki, C. W. W. Pirk, H. Human, Effects of a neonicotinoid pesticide on thermoregulation of African honey bees (*Apis mellifera scutellata*). *J. Insect Physiol.* **93-94**, 56–63 (2016). doi:10.1016/j.jinsphys.2016.08.010 Medline

19. R. Potts, R. M. Clarke, S. E. Oldfield, L. K. Wood, N. Hempel de Ibarra, J. E. Cresswell, The effect of dietary neonicotinoid pesticides on non-flight thermogenesis in worker bumble bees (Bombus terrestris). *J. Insect Physiol.* **104**, 33–39 (2018). doi:10.1016/j.jinsphys.2017.11.006 Medline

20. S. M. Williamson, S. J. Willis, G. A. Wright, Exposure to neonicotinoids influences the motor function of adult worker honeybees. *Ecotoxicology* **23**, 1409–1418 (2014). doi:10.1007/s10646-014-1283-x Medline

21. P. Medrzycki, R. Montanari, L. Bortolotti, S. Maini, C. Porrini, Effects of imidacloprid administered in sub-lethal doses on honey bee behaviour. Laboratory tests. *Bull. Insectol.* **56**, 59–62 (2017).

22. S. Tosi, J. C. Nieh, A common neonicotinoid pesticide, thiamethoxam, alters honey bee activity, motor functions, and movement to light. *Sci. Rep.* **7**, 15132 (2017). doi:10.1038/s41598-017-15308-6 Medline

23. J. D. Crall, N. Gravish, A. M. Mountcastle, S. A. Combes, BEEtag: A Low-Cost, Image-Based Tracking System for the Study of Animal Behavior and Locomotion. *PLOS ONE* **10**, e0136487 (2015). doi:10.1371/journal.pone.0136487 Medline

24. J. D. Crall, N. Gravish, A. M. Mountcastle, S. D. Kocher, R. L. Oppenheimer, N. E. Pierce, S. A. Combes, Spatial fidelity of workers predicts collective response to disturbance in a social insect. *Nat. Commun.* **9**, 1201 (2018). doi:10.1038/s41467-018-03561-w Medline

25. N. Forfert, R. F. A. Moritz, Thiacloprid alters social interactions among honey bee workers (*Apis mellifera*). *J. Apic. Res.* **56**, 467–474 (2017). doi:10.1080/00218839.2017.1332542

26. M. Lambin, C. Armengaud, S. Raymond, M. Gauthier, Imidacloprid-induced facilitation of the proboscis extension reflex habituation in the honeybee. *Arch. Insect Biochem. Physiol.* **48**, 129–134 (2001). doi:10.1002/arch.1065 Medline

27. J. Wu-Smart, M. Spivak, Sub-lethal effects of dietary neonicotinoid insecticide exposure on honey bee queen fecundity and colony development. *Sci. Rep.* **6**, 32108 (2016). doi:10.1038/srep32108 Medline

28. M. Leza, K. M. Watrous, J. Bratu, S. H. Woodard, Effects of neonicotinoid insecticide exposure and monofloral diet on nest-founding bumblebee queens. *Proc. Biol. Sci.* **285**, 20180761–20180769 (2018). doi:10.1098/rspb.2018.0761 Medline

29. G. L. Baron, N. E. Raine, M. J. F. Brown, General and species-specific impacts of a neonicotinoid insecticide on the ovary development and feeding of wild bumblebee queens. *Proc. Biol. Sci.* **284**, 20170123 (2017). doi:10.1098/rspb.2017.0123 Medline

30. J. G. Holland, A. F. G. Bourke, Colony and individual life-history responses to temperature in a social insect pollinator. *Funct. Ecol.* **29**, 1209–1217 (2015). doi:10.1111/1365-2435.12480

31. N. Tsvetkov, O. Samson-Robert, K. Sood, H. S. Patel, D. A. Malena, P. H. Gajiwala, P. Maciukiewicz, V. Fournier, A. Zayed, Chronic exposure to neonicotinoids reduces honey bee health near corn crops. *Science* **356**, 1395–1397 (2017). doi:10.1126/science.aam7470 Medline

32. J. D. Crall, C. M. Switzer, R. L. Oppenheimer, A. N. Ford Versypt, B. Dey, A. Brown, M. Eyster, C. Guérin, N. E. Pierce, S. A. Combes, B. L. de Bivort, Neonicotinoid exposure disrupts bumblebee nest behavior, social networks, and thermoregulation. Zenodo (2018); doi:10.5281/zenodo.1456183.

33. T. Alisch, J. D. Crall, A. B. Kao, D. Zucker, B. L. de Bivort, MAPLE (modular automated platform for large-scale experiments), a robot for integrated organism-handling and phenotyping. *eLife* **7**, e37166 (2018). doi:10.7554/eLife.37166 Medline

34. J. M. Jandt, E. Huang, A. Dornhaus, Weak specialization of workers inside a bumble bee (Bombus impatiens) nest. *Behav. Ecol. Sociobiol.* **63**, 1829–1836 (2009). doi:10.1007/s00265-009-0810-x

35. S. A. Cameron, Temporal Patterns of Division of Labor among Workers in the Primitively Eusocial Bumble Bee, Bombus griseocollis (Hymenoptera: Apidae)1). *Ethology* **80**, 137–151 (1989). doi:10.1111/j.1439-0310.1989.tb00735.x

36. M. A. Renner, J. C. Nieh, Bumble bee olfactory information flow and contact-based foraging activation. *Insectes Soc.* **55**, 417–424 (2008). doi:10.1007/s00040-008-1021-6

37. M. C. Otterstatter, J. D. Thomson, Contact networks and transmission of an intestinal pathogen in bumble bee (Bombus impatiens) colonies. *Oecologia* **154**, 411–421 (2007). doi:10.1007/s00442-007-0834-8 Medline

38. W. Zheng, W.-P. Liu, Y.-Z. Wen, S.-J. Lee, Photochemistry of insecticide imidacloprid: Direct and sensitized photolysis in aqueous medium. *J. Environ. Sci. (China)* **16**, 539–542 (2004). Medline

39. J. E. Cresswell, F.-X. L. Robert, H. Florance, N. Smirnoff, Clearance of ingested neonicotinoid pesticide (imidacloprid) in honey bees (*Apis mellifera*) and bumblebees (*Bombus terrestris*). *Pest Manag. Sci.* **70**, 332–337 (2014). doi:10.1002/ps.3569 Medline

40. P. Skorupski, L. Chittka, Photoreceptor spectral sensitivity in the bumblebee, *Bombus impatiens* (Hymenoptera: Apidae). *PLOS ONE* **5**, e12049 (2010). doi:10.1371/journal.pone.0012049 Medline

41. G. Csárdi, T. Nepusz, The igraph software package for complex network research. InterJournal Complex Systems 1695 (2006) (Springer Berlin Heidelberg, Berlin, Heidelberg, 2014).

42. P. Filzmoser, M. Gschwandtner, mvoutlier: Multivariate outlier detection based on robust methods (R package version, 2012).

43. J. P. Verma, *Repeated Measures Design for Empirical Researchers* (Wiley, 2015).

44. G. Heinze, M. Ploner, D. Dunkler, H. Southworth, logistf: Firth's bias reduced logistic regression (R package version, 2013).

45. S. Wood, F. Scheipl, Package 'gamm4'. *Am. Stat.* **45**, 339 (2017).

46. A. N. Ford Versypt, J. D. Crall, B. Dey, BeeNestABM: An open-source agent-based model of spatiotemporal distribution of bumblebees in nests. *J. Open Source Software* **3**, 718 (2018). doi:10.21105/joss.00718

47. J. C. Tuthill, R. I. Wilson, Parallel Transformation of Tactile Signals in Central Circuits of *Drosophila*. *Cell* **164**, 1046–1059 (2016). doi:10.1016/j.cell.2016.01.014 Medline

48. H. C. J. Godfray, T. Blacquière, L. M. Field, R. S. Hails, S. G. Potts, N. E. Raine, A. J. Vanbergen, A. R. McLean, A restatement of recent advances in the natural science evidence base concerning neonicotinoid insecticides and insect pollinators. *Proc. Biol. Sci.* **282**, 20151821 (2015). doi:10.1098/rspb.2015.1821 Medline

49. F. J. Byrne, P. K. Visscher, B. Leimkuehler, D. Fischer, E. E. Grafton-Cardwell, J. G. Morse, Determination of exposure levels of honey bees foraging on flowers of mature citrus trees previously treated with imidacloprid. *Pest Manag. Sci.* **70**, 470–482 (2014). doi:10.1002/ps.3596 Medline

50. K. A. Stoner, B. D. Eitzer, Movement of soil-applied imidacloprid and thiamethoxam into nectar and pollen of squash (*Cucurbita pepo*). *PLOS ONE* **7**, e39114 (2012). doi:10.1371/journal.pone.0039114 Medline

51. V. A. Krischik, A. L. Landmark, G. E. Heimpel, Soil-applied imidacloprid is translocated to nectar and kills nectar-feeding *Anagyrus pseudococci* (Girault) (Hymenoptera: Encyrtidae). *Environ. Entomol.* **36**, 1238–1245 (2007). doi:10.1603/0046-225X(2007)36[1238:SIITTN]2.0.CO;2 Medline

52. C. Botías, A. David, E. M. Hill, D. Goulson, Quantifying exposure of wild bumblebees to mixtures of agrochemicals in agricultural and urban landscapes. *Environ. Pollut.* **222**, 73–82 (2017). doi:10.1016/j.envpol.2017.01.001 Medline

53. C. Botías, A. David, J. Horwood, A. Abdul-Sada, E. Nicholls, E. Hill, D. Goulson, Neonicotinoid Residues in Wildflowers, a Potential Route of Chronic Exposure for Bees. *Environ. Sci. Technol.* **49**, 12731–12740 (2015). doi:10.1021/acs.est.5b03459 Medline

54. S. Suchail, D. Guez, L. P. Belzunces, Discrepancy between acute and chronic toxicity induced by imidacloprid and its metabolites in *Apis mellifera*. *Environ. Toxicol. Chem.* **20**, 2482–2486 (2001). doi:10.1897/1551-5028(2001)020<2482:DBAACT>2.0.CO;2 Medline